

Bayesian Compressive Imaging of Non-Weak Scatterers through the Born Iterative Method

G. Oliveri, L. Poli, N. Anselmi, M. Salucci, and A. Massa

Abstract

This work deals with the problem of imaging non-weak scatterers in the Compressive Sensing (CS) framework. Towards this end, an innovative hybrid Born Iterative Compressive Sensing method has been developed, by suitably formulating the non-linear inverse scattering (IS) problem at hand within the Born Iterative (BI) framework and exploiting a customized version of the single-task Bayesian CS (ST-BCS) solution method. Selected numerical results are shown to assess the potentialities of the proposed IS methodology when dealing with several types of unknown scatterers and processing noisy data with different signal-to-noise ratios.

Contents

1	Numerical Results	3
1.1	Rectangular-shaped Object $\ell = \lambda/6, h = \lambda/4$	3
1.1.1	Rectangle-shaped Object, $\ell = \lambda/6, h = \lambda/4$, - ST-BCS reconstructed profiles with first Born approximation	5
1.1.2	Rectangle-shaped Object, $\ell = \lambda/6, h = \lambda/4$, - ST-BCS reconstructed profiles with Born Iterative Method ($I_{MAX} = 10$)	6
1.1.3	Rectangle-shaped Object, $\ell = \lambda/6, h = \lambda/4$, - ST-BCS reconstructed profiles with Born Iterative Method (Threshold η)	9
1.2	Square-shaped Object, $\ell = \lambda/4$	10
1.2.1	Square-shaped Object, $\ell = \lambda/4$ - ST-BCS reconstructed profiles with first Born approximation	12
1.2.2	Square-shaped Object, $\ell = \lambda/4$ - ST-BCS reconstructed profiles with Born Iterative Method ($I_{MAX} = 10$)	13
1.2.3	Square-shaped Object, $\ell = \lambda/4$ - ST-BCS reconstructed profiles with Born Iterative Method (Threshold η)	16
1.3	Square-shaped Object, $\ell = \lambda/3$	17
1.3.1	Square-shaped Object, $\ell = \lambda/3$ - ST-BCS reconstructed profiles with first Born approximation	19
1.3.2	Square-shaped Object, $\ell = \lambda/3$ - ST-BCS reconstructed profiles with Born Iterative Method ($I_{MAX} = 10$)	20
1.3.3	Square-shaped Object, $\ell = \lambda/3$ - ST-BCS reconstructed profiles with Born Iterative Method (Threshold η)	23
1.4	L-shaped Object, $\ell = \lambda/2$	24
1.4.1	L-shaped Object, $\ell = \lambda/2 - \tau = 0.5$	26
1.4.2	L-shaped Object, $\ell = \lambda/2 - \tau = 1.0$	27
1.4.3	L-shaped Object, $\ell = \lambda/2 - \tau = 2.0$	28
1.5	E-shaped Object, $\ell_1 = \frac{5}{6}\lambda, \ell_2 = \lambda/2$	29
1.5.1	E-shaped Object, $\ell_1 = \frac{5}{6}\lambda, \ell_2 = \lambda/2 - \tau = 0.5$	31
1.5.2	E-shaped Object, $\ell_1 = \frac{5}{6}\lambda, \ell_2 = \lambda/2 - \tau = 1.0$	32
1.5.3	E-shaped Object, $\ell_1 = \frac{5}{6}\lambda, \ell_2 = \lambda/2 - \tau = 2.0$	33
1.6	C-shaped Object, $\ell_1 = \frac{2}{3}\lambda, \ell_2 = \lambda/2$	34
1.6.1	C-shaped Object, $\ell_1 = \frac{2}{3}\lambda, \ell_2 = \lambda/2 - \tau = 0.5$	36
1.6.2	C-shaped Object, $\ell_1 = \frac{2}{3}\lambda, \ell_2 = \lambda/2 - \tau = 1.0$	37

1.6.3	C-shaped Object, $\ell_1 = \frac{2}{3}\lambda$, $\ell_2 = \lambda/2 - \tau = 2.0$	38
1.7	Rectangle-shaped Object, $\ell = \lambda/2$, $h = \lambda/3$	39
1.7.1	Rectangle-shaped Object, $\ell = \lambda/2$, $h = \lambda/3 - \tau = 0.5$	41
1.7.2	Rectangle-shaped Object, $\ell = \lambda/2$, $h = \lambda/3 - \tau = 1.0$	42
1.7.3	Rectangle-shaped Object, $\ell = \lambda/2$, $h = \lambda/3 - \tau = 2.0$	43
1.8	Multiple Objects	44
1.8.1	Multiple Objects, $\tau = 0.5$	46
1.8.2	Multiple Object, $\tau = 1.0$	47
1.8.3	Multiple Objects, $\tau = 2.0$	48

ELEDIA Research Center

1 Numerical Results

1.1 Rectangular-shaped Object $\ell = \lambda/6, h = \lambda/4$

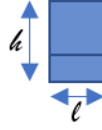


Figure 1: Rectangle-shaped Object

Test Case Description

Direct solver:

- Cubic domain divided in $\sqrt{D} \times \sqrt{D}$ cells
- Number of cells for the direct solver: $D = 1296$ (discretization = $\lambda/12$)

Inverse solver:

- Cubic domain divided in $\sqrt{N} \times \sqrt{N}$ cells
- Number of cells for the inversion: $N = 324$ (discretization = $\lambda/6$)

Measurement domain:

- Total number of measurements: $M = 27$
- Measurement points placed on circles of radius $\rho = 3\lambda$

Sources:

- Plane waves
- Number of views: $V = 27; \theta_{inc}^v = 0^\circ + (v - 1) \times (360/V)$
- Amplitude: $A = 1.0$
- Frequency: $F = 300$ MHz ($\lambda = 1$)

Background:

- $\varepsilon_r = 1.0$
- $\sigma = 0$ [S/m]

Scatterer

- Rectangle-shaped object, $\ell = \lambda/6$, $h = \lambda/4$
- $\varepsilon_r \in 4.0$
- $\sigma = 0$ [S/m]

Born Iterative Method

- $I_{MAX} = 10$
- $\eta = 10^{-3}$

ELEDIA Research Center

1.1.1 Rectangle-shaped Object, $\ell = \lambda/6$, $h = \lambda/4$, - ST-BCS reconstructed profiles with first Born approximation

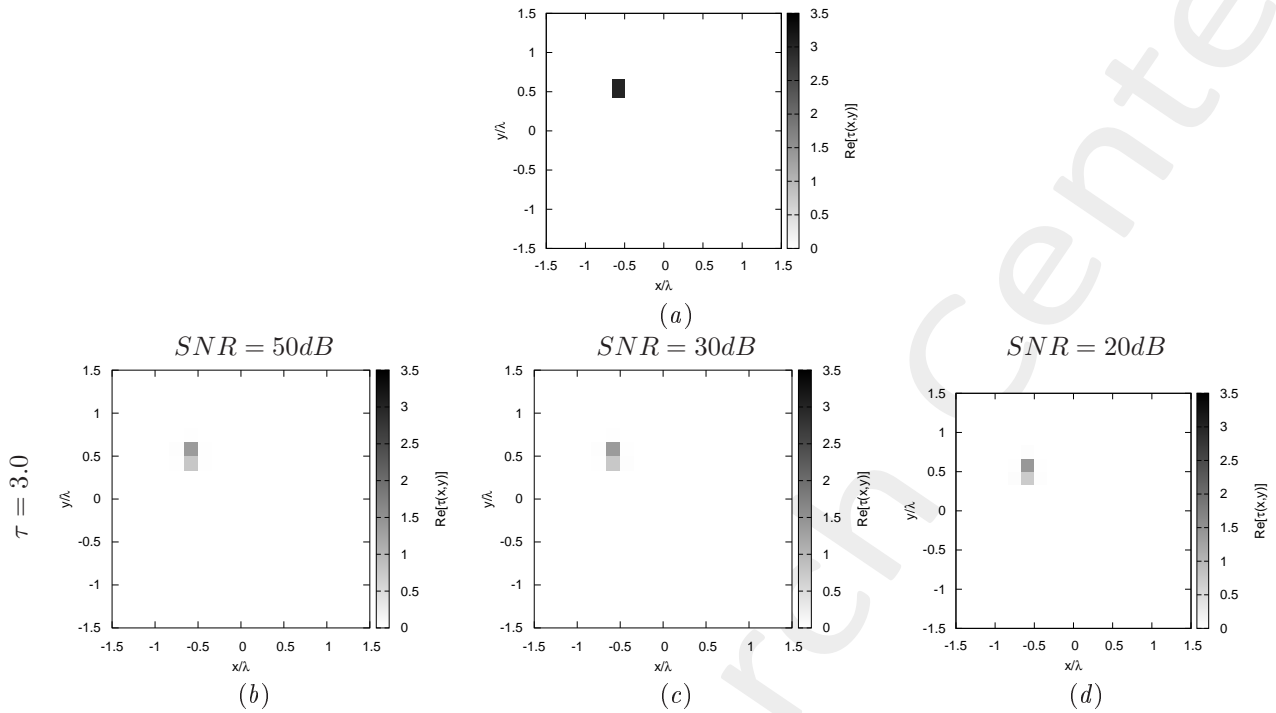


Figure 2: *Rectangle-shaped Object*, $\ell = \lambda/6$, $h = \lambda/4$: (a) Direct problem with $\tau = 3.0$, (b) ST-BCS reconstructed profiles for $\text{SNR} = 50$ [dB], (c) $\text{SNR} = 30$ [dB] and (d) $\text{SNR} = 20$ [dB]

1.1.2 Rectangle-shaped Object, $\ell = \lambda/6$, $h = \lambda/4$, - ST-BCS reconstructed profiles with Born Iterative Method ($I_{MAX} = 10$)

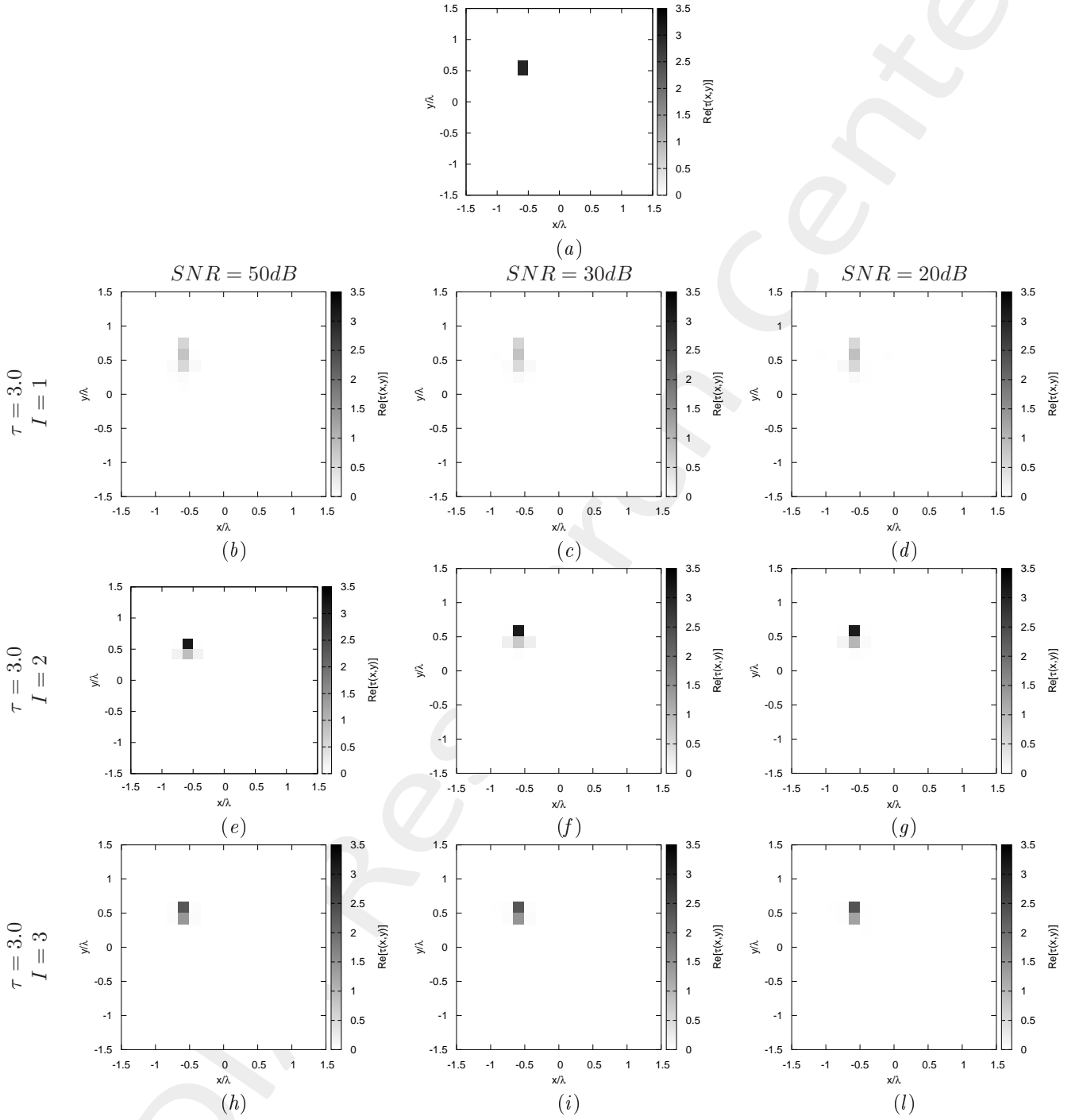


Figure 3: *Rectangle-shaped Object*, $\ell = \lambda/6$, $h = \lambda/4$: (a) Direct problem with $\tau = 3.0$, (b)(e)(h) ST-BCS reconstructed profiles for $\text{SNR} = 50$ [dB], (c)(f)(i) $\text{SNR} = 30$ [dB] and (d)(g)(l) $\text{SNR} = 20$ [dB] with (b)-(d) Born Iterative Method at the first iteration ($I = 1$), (e)-(g) Born Iterative Method at the second iteration ($I = 2$), (h)-(l) Born Iterative Method at the third iteration ($I = 3$)

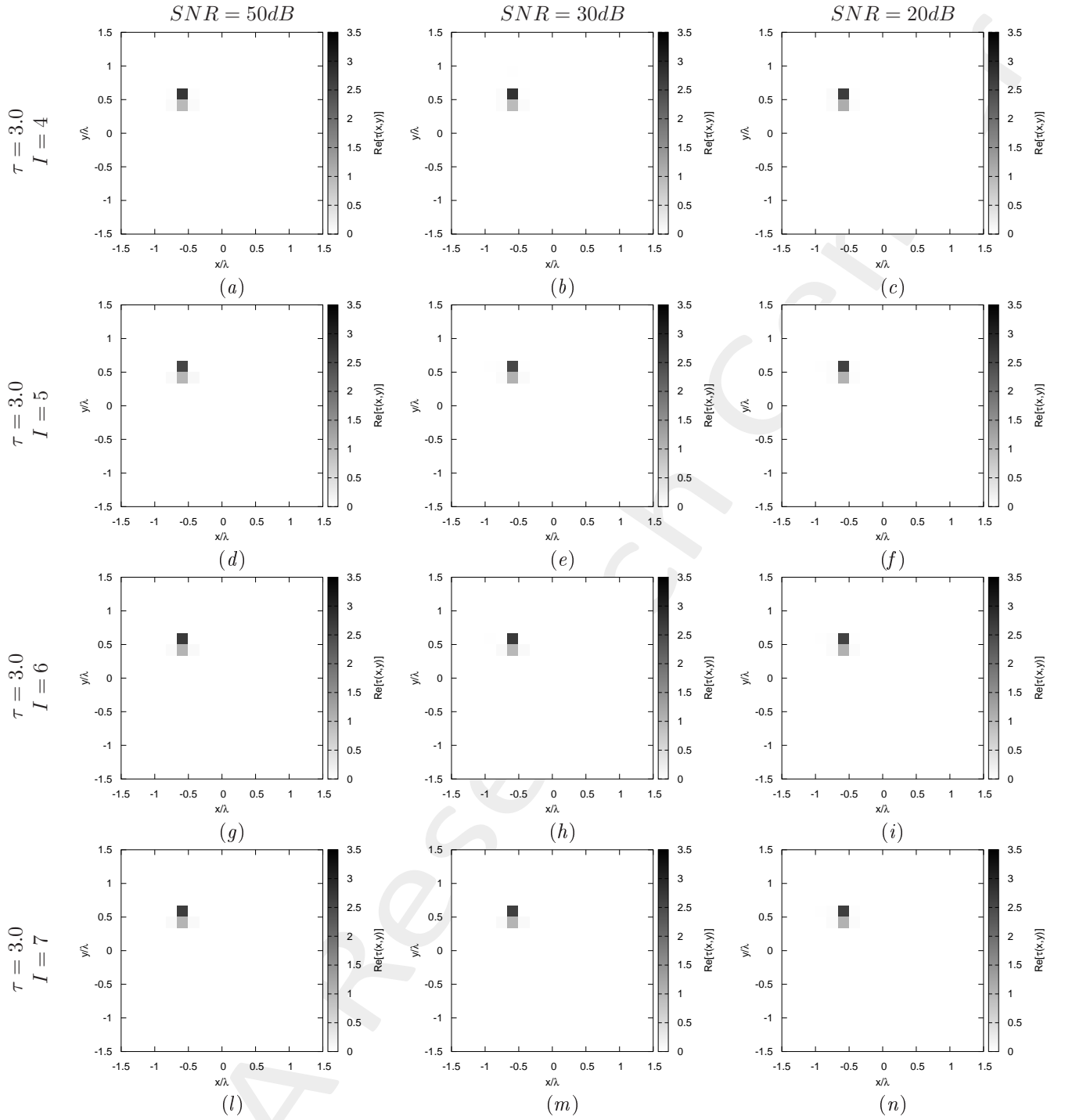


Figure 4: *Rectangle-shaped Object*, $\ell = \lambda/6$, $h = \lambda/4$: (a)(d)(g)(l) ST-BCS reconstructed profiles for $SNR = 50$ [dB], (b)(e)(h)(m) $SNR = 30$ [dB] and (c)(f)(i)(n) $SNR = 20$ [dB] with (a)-(c) Born Iterative Method at the fourth iteration ($I = 4$), (d)-(f) Born Iterative Method at the fifth iteration ($I = 5$), (g)-(i) Born Iterative Method at the sixth iteration ($I = 6$), (l)-(n) Born Iterative Method at the seventh iteration ($I = 7$)

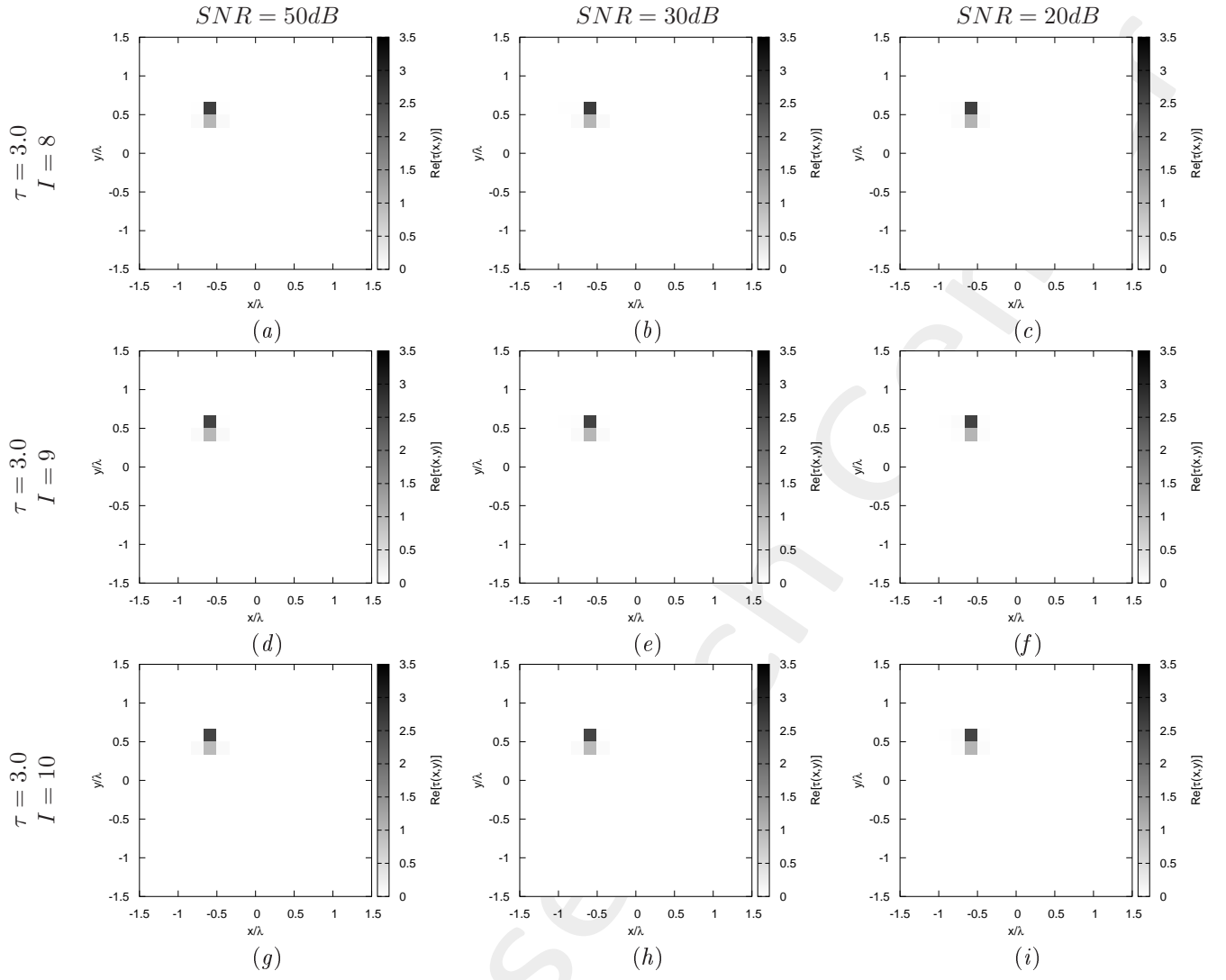


Figure 5: *Rectangle-shaped Object*, $\ell = \lambda/6$, $h = \lambda/4$: (a)(d)(g)(l) ST-BCS reconstructed profiles for $SNR = 50$ [dB], (b)(e)(h)(m) $SNR = 30$ [dB] and (c)(f)(i)(n) $SNR = 20$ [dB] with (a)-(c) Born Iterative Method at the eighth iteration ($I = 8$), (d)-(f) Born Iterative Method at the ninth iteration ($I = 9$), (g)-(i) Born Iterative Method at the tenth iteration ($I = 10$)

1.1.3 Rectangle-shaped Object, $\ell = \lambda/6$, $h = \lambda/4$, - ST-BCS reconstructed profiles with Born Iterative Method (Threshold η)

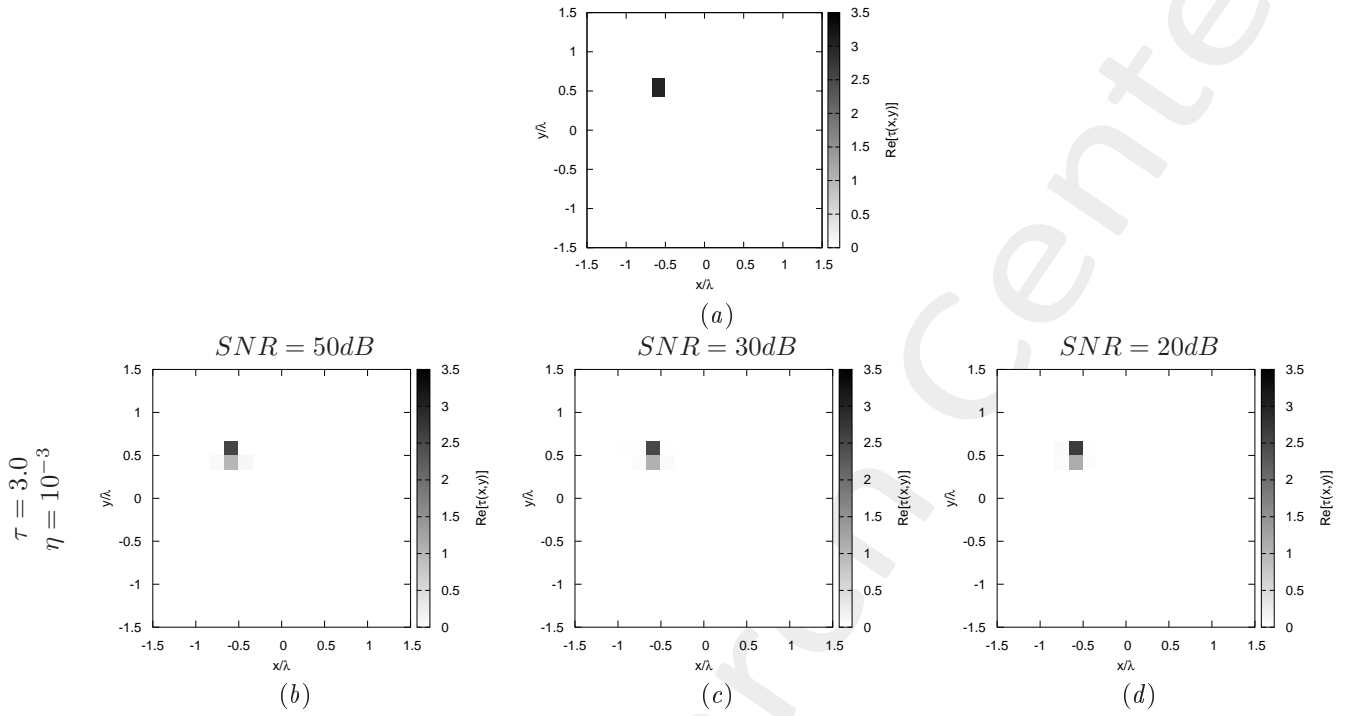


Figure 6: *Rectangle-shaped Object*, $\ell = \lambda/6$, $h = \lambda/4$: (a) Direct problem with $\tau = 3.0$, (b) ST-BCS reconstructed profiles for $\text{SNR} = 50$ [dB], (c) $\text{SNR} = 30$ [dB] and (d) $\text{SNR} = 20$ [dB] with (b)-(d) Born Iterative Method with threshold $\eta = 10^{-3}$

1.2 Square-shaped Object, $\ell = \lambda/4$

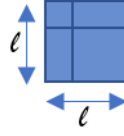


Figure 7: Square-shaped Object

Test Case Description

Direct solver:

- Cubic domain divided in $\sqrt{D} \times \sqrt{D}$ cells
- Number of cells for the direct solver: $D = 1296$ (discretization = $\lambda/12$)

Inverse solver:

- Cubic domain divided in $\sqrt{N} \times \sqrt{N}$ cells
- Number of cells for the inversion: $N = 324$ (discretization = $\lambda/6$)

Measurement domain:

- Total number of measurements: $M = 27$
- Measurement points placed on circles of radius $\rho = 3\lambda$

Sources:

- Plane waves
- Number of views: $V = 27$; $\theta_{inc}^v = 0^\circ + (v - 1) \times (360/V)$
- Amplitude: $A = 1.0$
- Frequency: $F = 300$ MHz ($\lambda = 1$)

Background:

- $\varepsilon_r = 1.0$
- $\sigma = 0$ [S/m]

Scatterer

- Square-shaped object, $\ell = \lambda/4$
- $\varepsilon_r \in 3.0$
- $\sigma = 0$ [S/m]

Born Iterative Method

- $I_{MAX} = 10$
- $\eta = 10^{-3}$

ELEDIA Research Center

1.2.1 Square-shaped Object, $\ell = \lambda/4$ - ST-BCS reconstructed profiles with first Born approximation

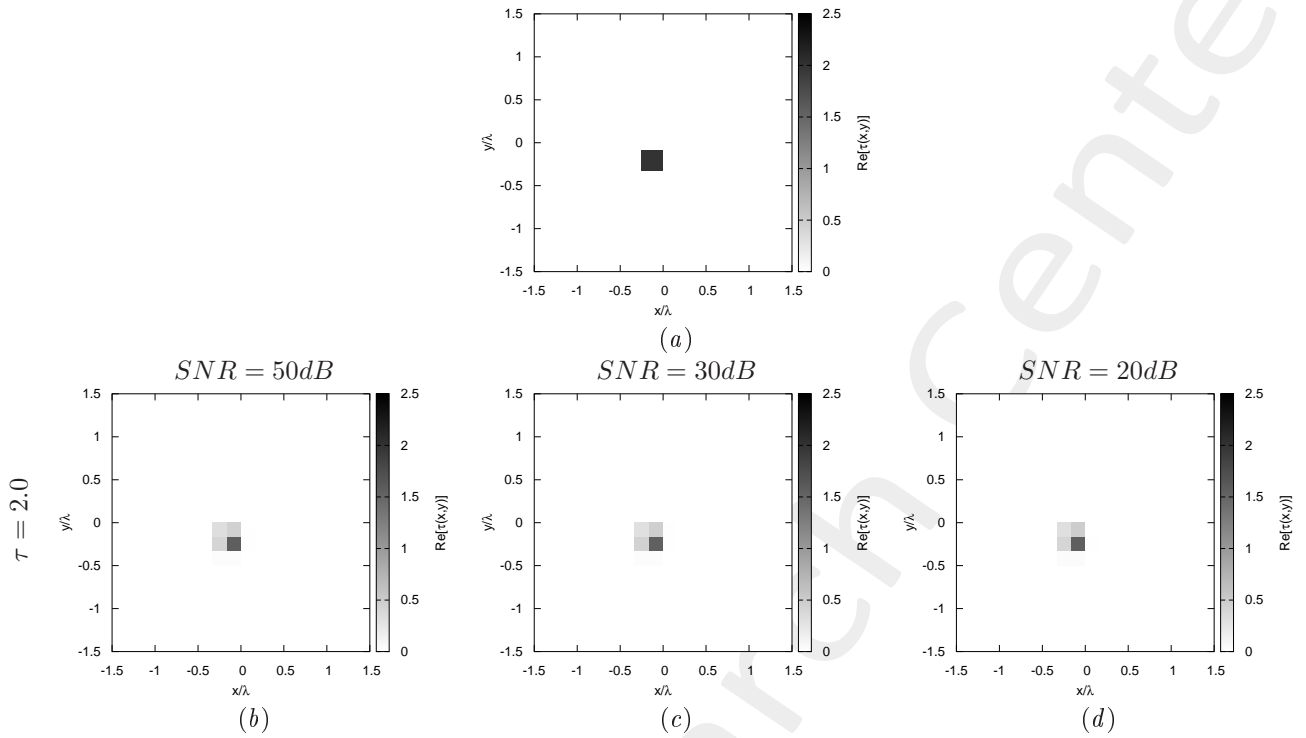


Figure 8: *Square-shaped Object*, $\ell = \lambda/4$: (a) Direct problem with $\tau = 2.0$, (b) ST-BCS reconstructed profiles for $\text{SNR} = 50$ [dB], (c) $\text{SNR} = 30$ [dB] and (d) $\text{SNR} = 20$ [dB]

1.2.2 Square-shaped Object, $\ell = \lambda/4$ - ST-BCS reconstructed profiles with Born Iterative Method

($I_{MAX} = 10$)

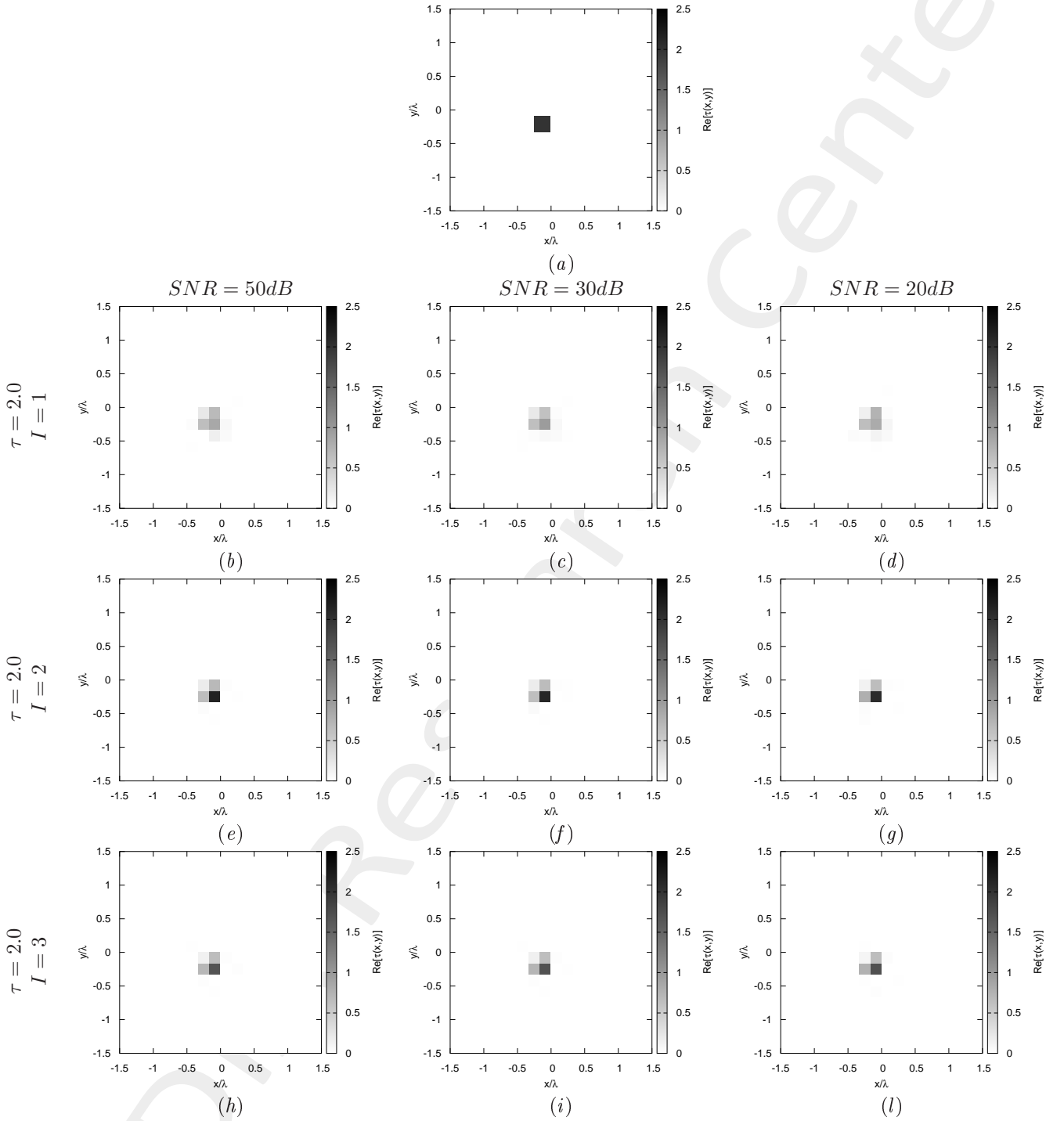


Figure 9: *Square-shaped Object*, $\ell = \lambda/4$: (a) Direct problem with $\tau = 2.0$, (b)(e)(h) ST-BCS reconstructed profiles for $SNR = 50$ [dB], (c)(f)(i) $SNR = 30$ [dB] and (d)(g)(l) $SNR = 20$ [dB] with (b)-(d) Born Iterative Method at the first iteration ($I = 1$), (e)-(g) Born Iterative Method at the second iteration ($I = 2$), (h)-(l) Born Iterative Method at the third iteration ($I = 3$)

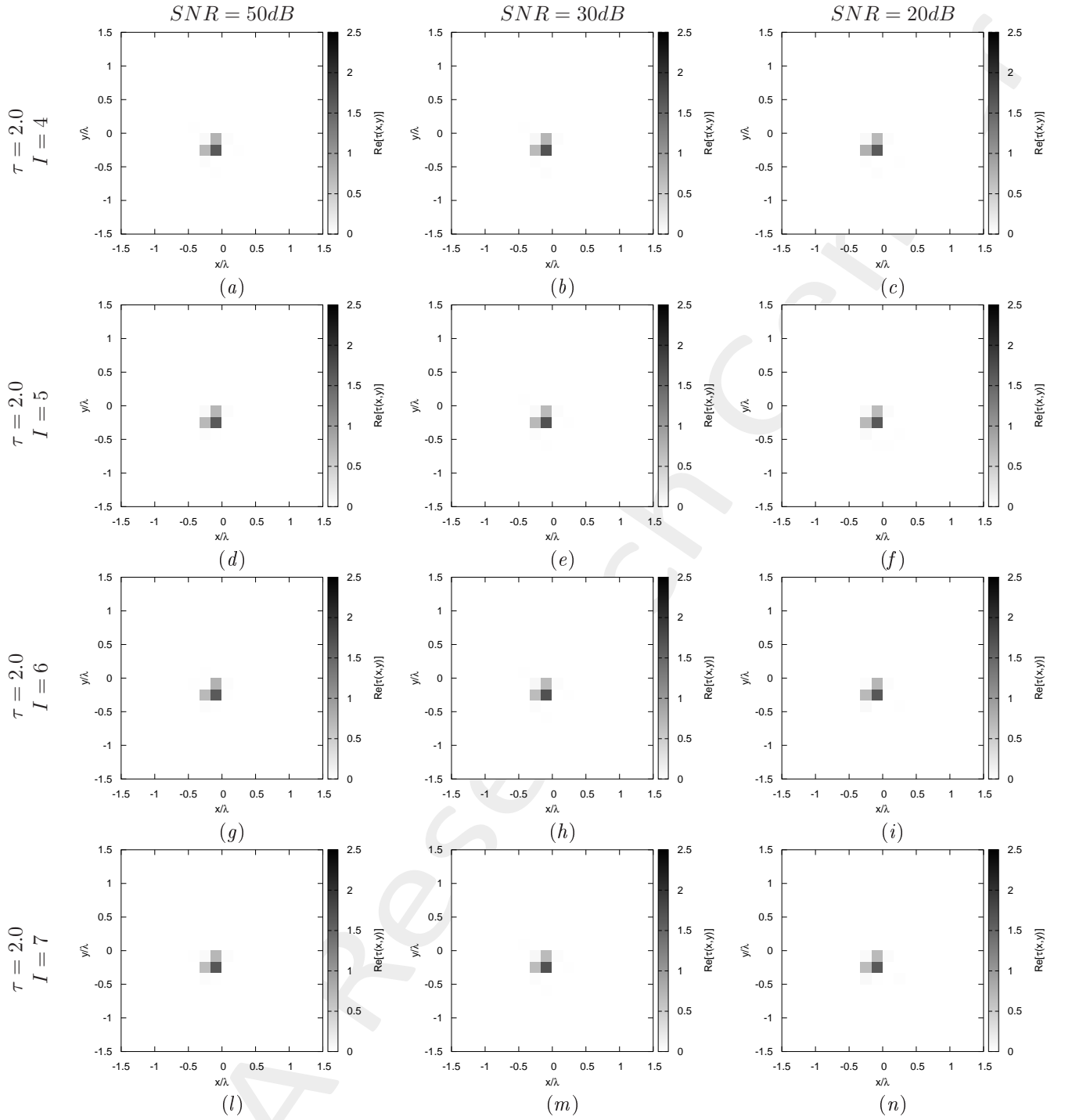


Figure 10: *Square-shaped Object*, $\ell = \lambda/4$: (a)(d)(g)(l) ST-BCS reconstructed profiles for $SNR = 50$ [dB], (b)(e)(h)(m) $SNR = 30$ [dB] and (c)(f)(i)(n) $SNR = 20$ [dB] with (a)-(c) Born Iterative Method at the fourth iteration ($I = 4$), (d)-(f) Born Iterative Method at the fifth iteration ($I = 5$), (g)-(i) Born Iterative Method at the sixth iteration ($I = 6$), (l)-(n) Born Iterative Method at the seventh iteration ($I = 7$)

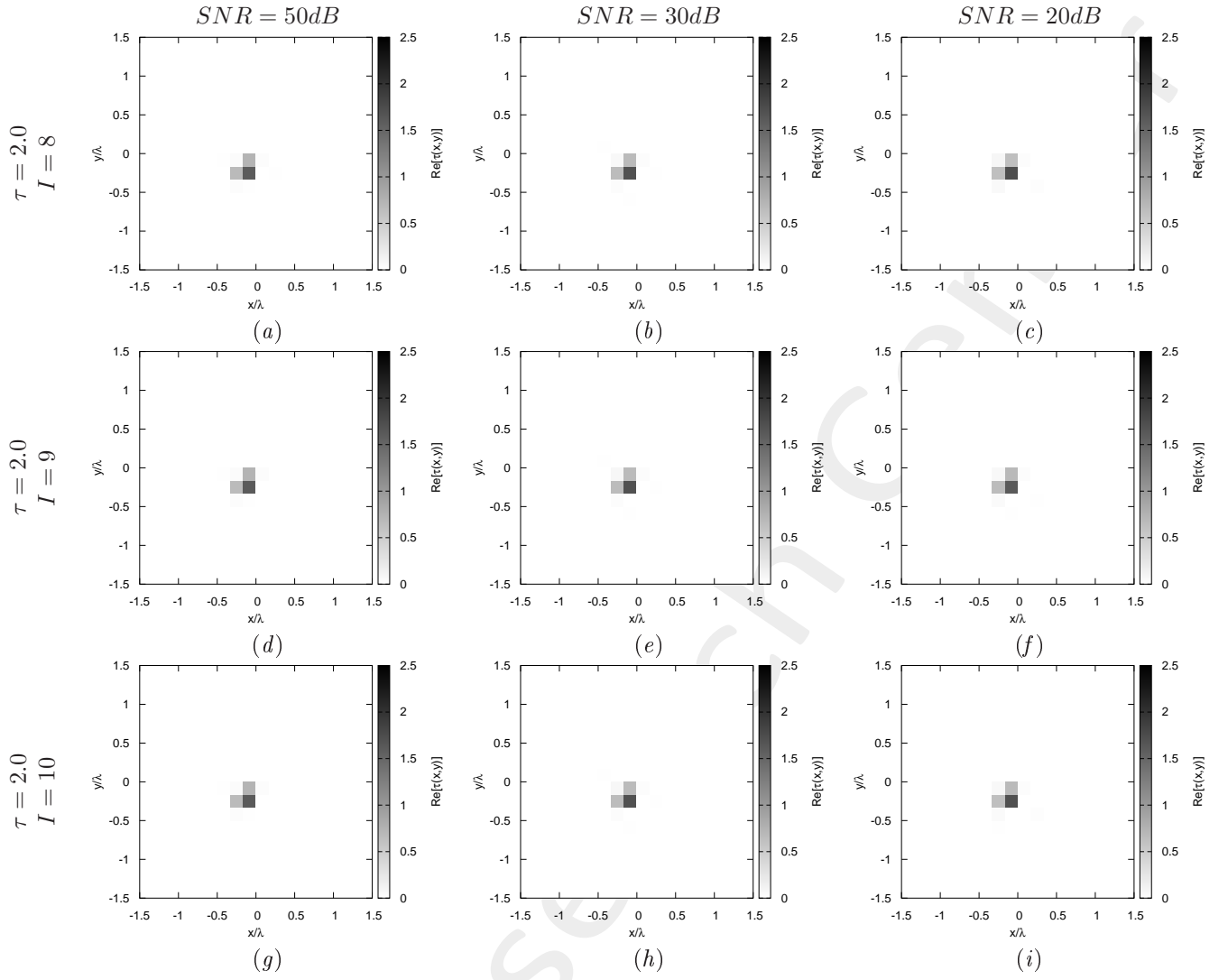


Figure 11: *Square-shaped Object*, $\ell = \lambda/4$: (a)(d)(g)(l) ST-BCS reconstructed profiles for $SNR = 50$ [dB], (b)(e)(h)(m) $SNR = 30$ [dB] and (c)(f)(i)(n) $SNR = 20$ [dB] with (a)-(c) Born Iterative Method at the eighth iteration ($I = 8$), (d)-(f) Born Iterative Method at the ninth iteration ($I = 9$), (g)-(i) Born Iterative Method at the tenth iteration ($I = 10$)

1.2.3 Square-shaped Object, $\ell = \lambda/4$ - ST-BCS reconstructed profiles with Born Iterative Method
(Threshold η)

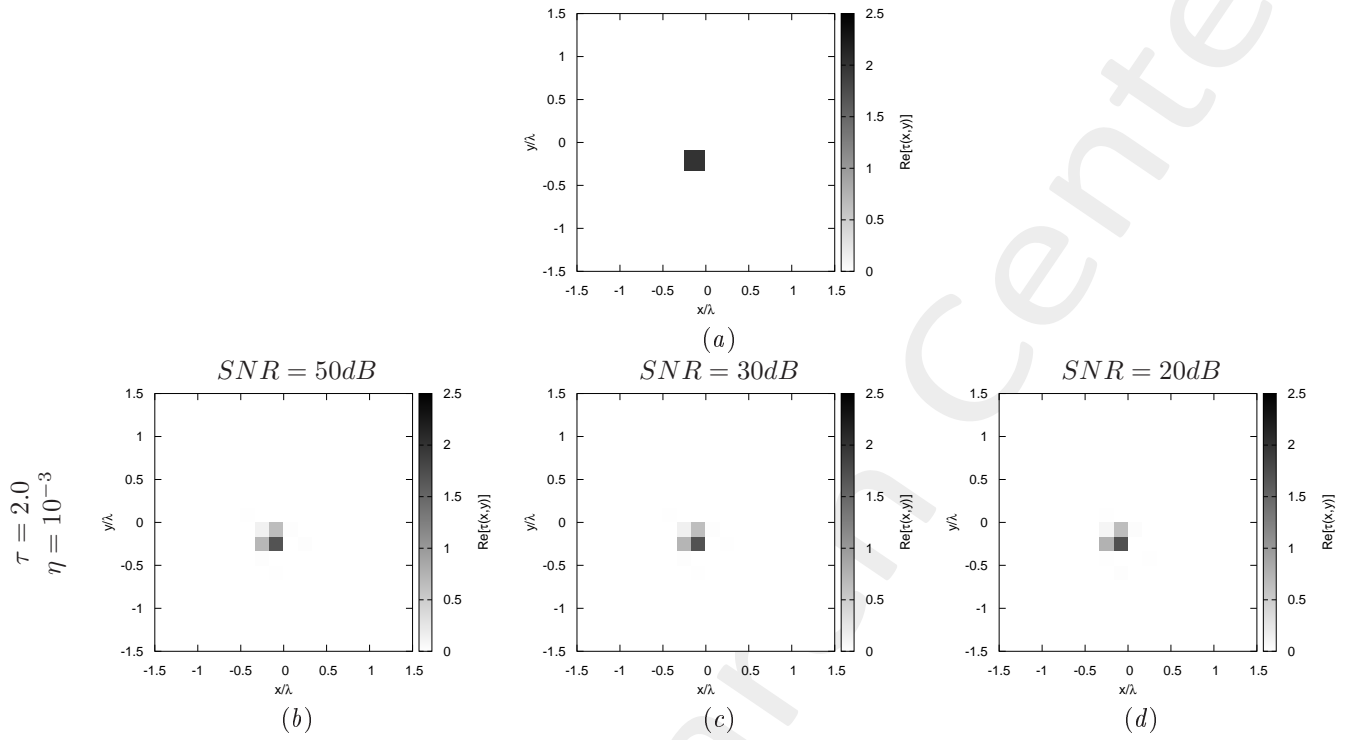


Figure 12: *Square-shaped Object*, $\ell = \lambda/4$: (a) Direct problem with $\tau = 2.0$, (b) ST-BCS reconstructed profiles for $SNR = 50$ [dB], (c) $SNR = 30$ [dB] and (d) $SNR = 20$ [dB] with (b)-(d) Born Iterative Method with threshold $\eta = 10^{-3}$

1.3 Square-shaped Object, $\ell = \lambda/3$

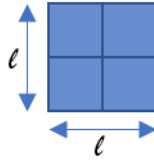


Figure 13: Square-shaped Object

Test Case Description

Direct solver:

- Cubic domain divided in $\sqrt{D} \times \sqrt{D}$ cells
- Number of cells for the direct solver: $D = 1296$ (discretization = $\lambda/12$)

Inverse solver:

- Cubic domain divided in $\sqrt{N} \times \sqrt{N}$ cells
- Number of cells for the inversion: $N = 324$ (discretization = $\lambda/6$)

Measurement domain:

- Total number of measurements: $M = 27$
- Measurement points placed on circles of radius $\rho = 3\lambda$

Sources:

- Plane waves
- Number of views: $V = 27$; $\theta_{inc}^v = 0^\circ + (v - 1) \times (360/V)$
- Amplitude: $A = 1.0$
- Frequency: $F = 300$ MHz ($\lambda = 1$)

Background:

- $\varepsilon_r = 1.0$
- $\sigma = 0$ [S/m]

Scatterer

- Square-shaped object, $\ell = \lambda/3$
- $\varepsilon_r \in 3.0$
- $\sigma = 0$ [S/m]

Born Iterative Method

- $I_{MAX} = 10$
- $\eta = 10^{-3}$

ELEDIA Research Center

1.3.1 Square-shaped Object, $\ell = \lambda/3$ - ST-BCS reconstructed profiles with first Born approximation

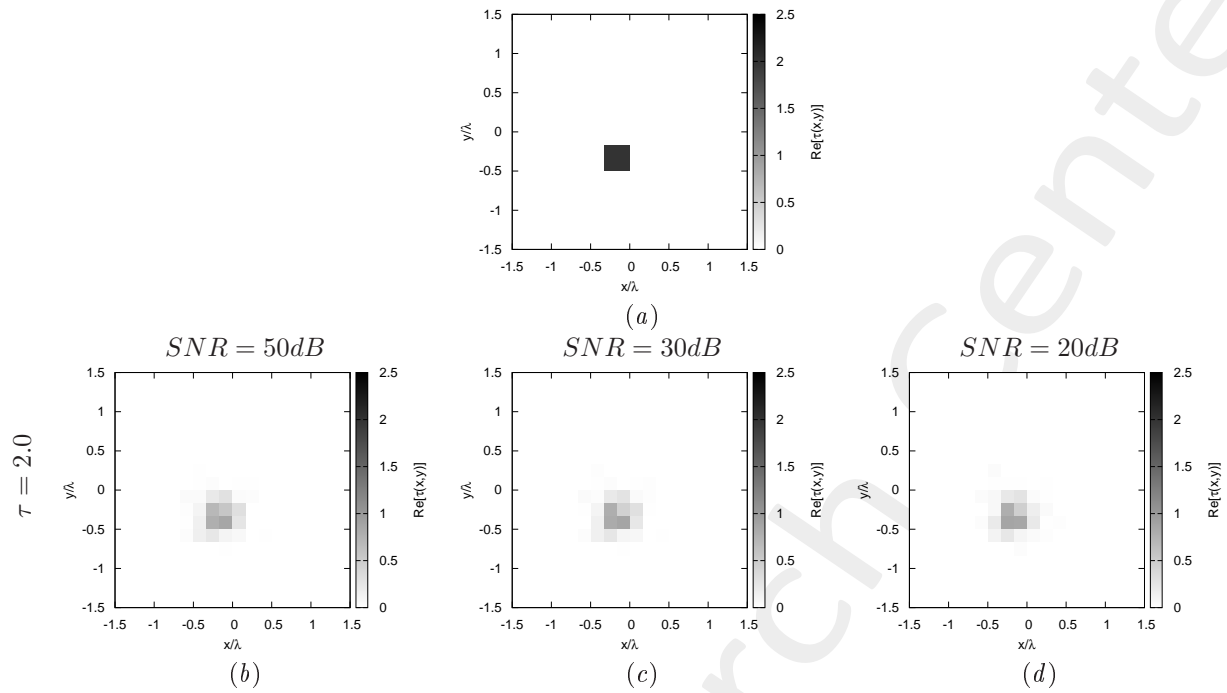


Figure 14: *Square-shaped Object*, $\ell = \lambda/3$: (a) Direct problem with $\tau = 2.0$, (b) ST-BCS reconstructed profiles for $SNR = 50$ [dB], (c) $SNR = 30$ [dB] and (d) $SNR = 20$ [dB]

1.3.2 Square-shaped Object, $\ell = \lambda/3$ - ST-BCS reconstructed profiles with Born Iterative Method

($I_{MAX} = 10$)

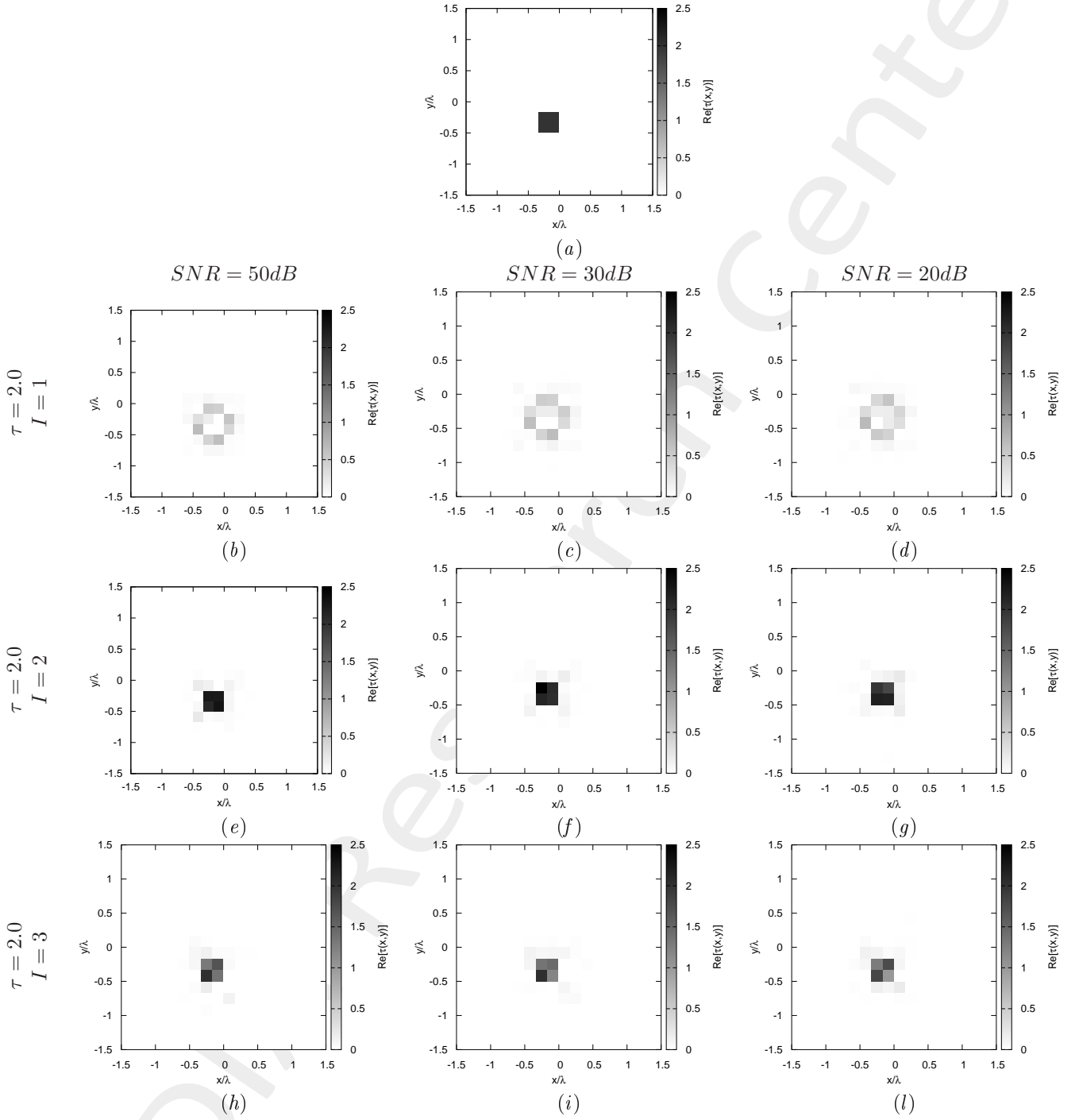


Figure 15: *Square-shaped Object, $\ell = \lambda/3$* : (a) Direct problem with $\tau = 2.0$, (b)(e)(h) ST-BCS reconstructed profiles for $SNR = 50$ [dB], (c)(f)(i) $SNR = 30$ [dB] and (d)(g)(l) $SNR = 20$ [dB] with (b)-(d) Born Iterative Method at the first iteration ($I = 1$), (e)-(g) Born Iterative Method at the second iteration ($I = 2$), (h)-(l) Born Iterative Method at the third iteration ($I = 3$)

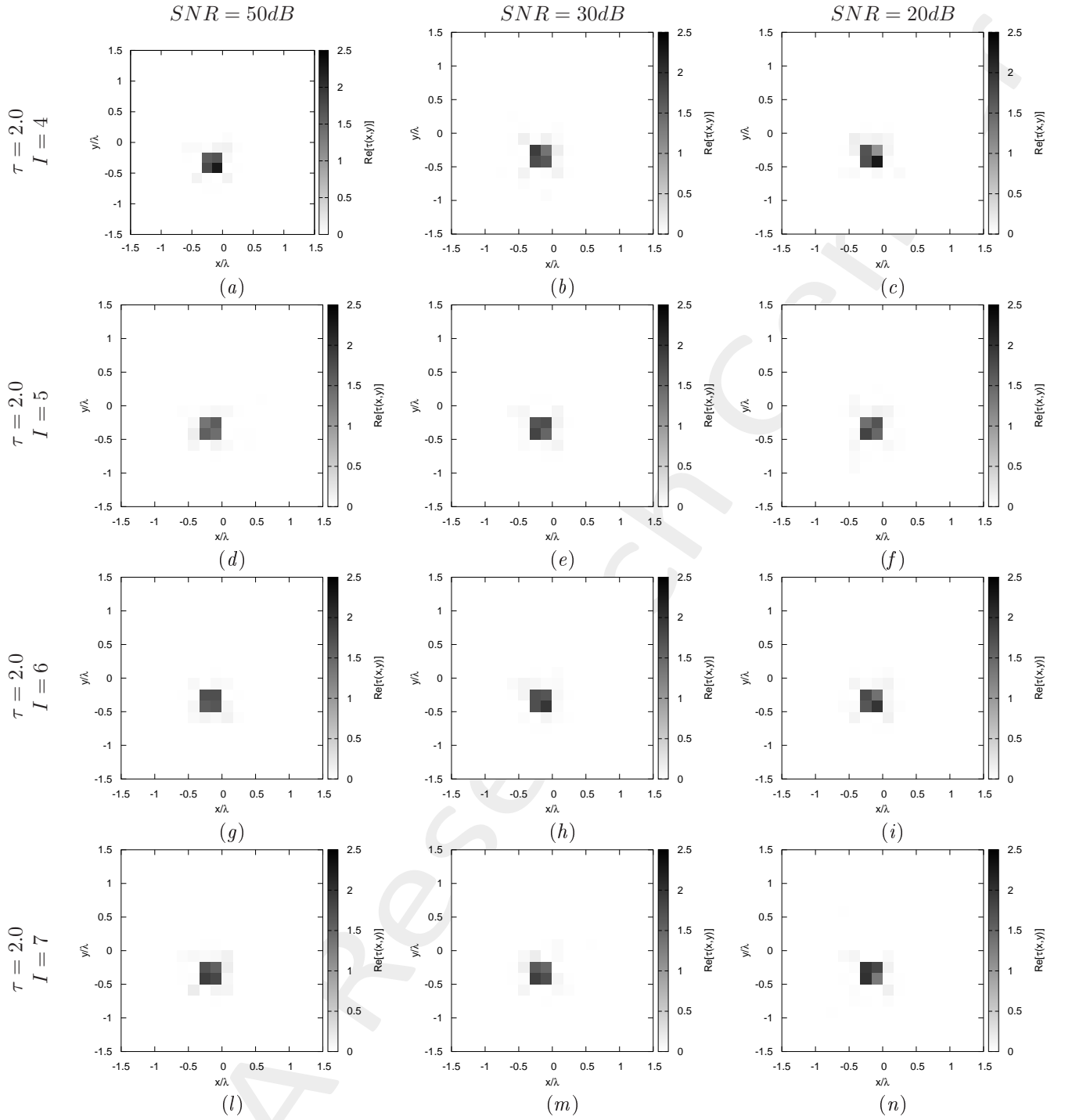


Figure 16: *Square-shaped Object*, $\ell = \lambda/3$: (a)(d)(g)(l) ST-BCS reconstructed profiles for $SNR = 50$ [dB], (b)(e)(h)(m) $SNR = 30$ [dB] and (c)(f)(i)(n) $SNR = 20$ [dB] with (a)-(c) Born Iterative Method at the fourth iteration ($I = 4$), (d)-(f) Born Iterative Method at the fifth iteration ($I = 5$), (g)-(i) Born Iterative Method at the sixth iteration ($I = 6$), (l)-(n) Born Iterative Method at the seventh iteration ($I = 7$)

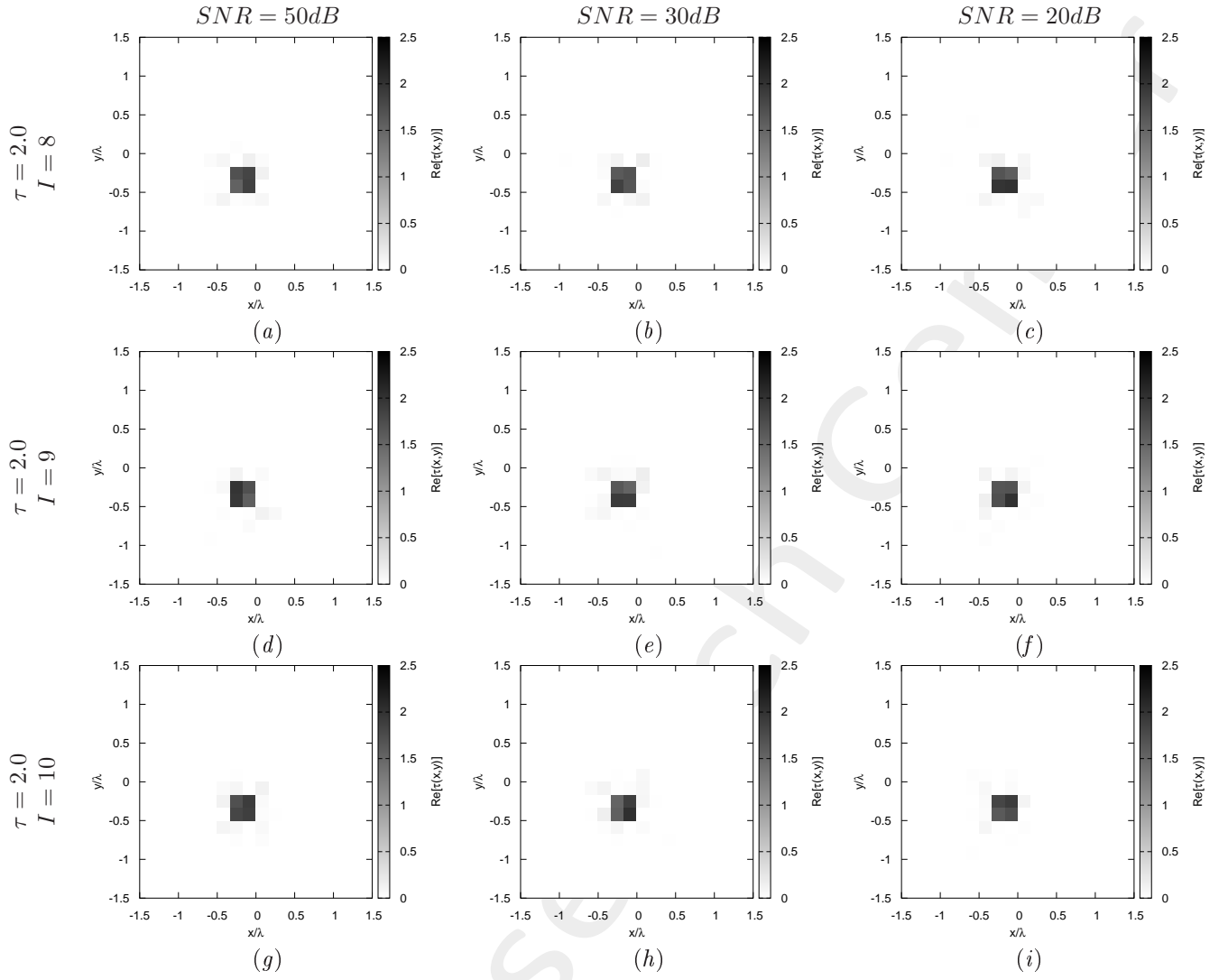


Figure 17: *Square-shaped Object*, $\ell = \lambda/3$: (a)(d)(g)(l) ST-BCS reconstructed profiles for $SNR = 50$ [dB], (b)(e)(h)(m) $SNR = 30$ [dB] and (c)(f)(i)(n) $SNR = 20$ [dB] with (a)-(c) Born Iterative Method at the eighth iteration ($I = 8$), (d)-(f) Born Iterative Method at the ninth iteration ($I = 9$), (g)-(i) Born Iterative Method at the tenth iteration ($I = 10$)

1.3.3 Square-shaped Object, $\ell = \lambda/3$ - ST-BCS reconstructed profiles with Born Iterative Method
(Threshold η)

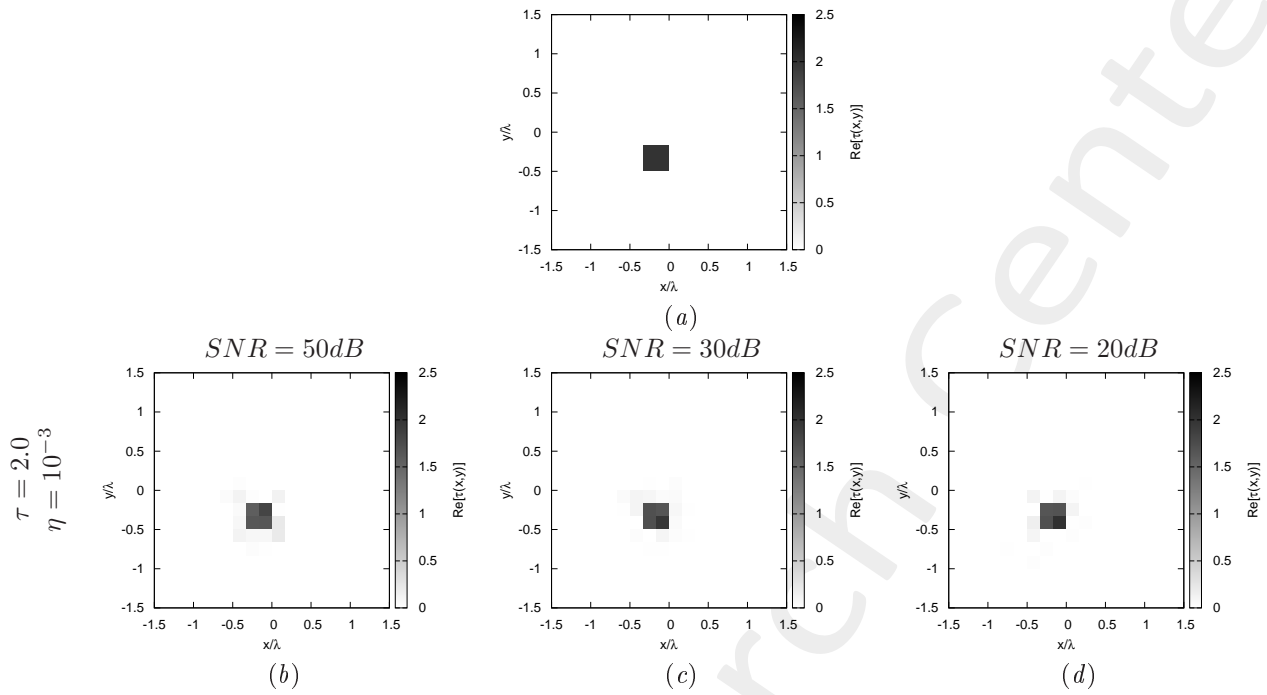


Figure 18: *Square-shaped Object*, $\ell = \lambda/3$: (a) Direct problem with $\tau = 2.0$, (b) ST-BCS reconstructed profiles for $SNR = 50$ [dB], (c) $SNR = 30$ [dB] and (d) $SNR = 20$ [dB] with (b)-(d) Born Iterative Method with threshold $\eta = 10^{-3}$

1.4 L-shaped Object, $\ell = \lambda/2$

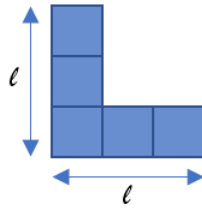


Figure 19: L-shaped Object

Test Case Description

Direct solver:

- Cubic domain divided in $\sqrt{D} \times \sqrt{D}$ cells
- Number of cells for the direct solver: $D = 1296$ (discretization = $\lambda/12$)

Inverse solver:

- Cubic domain divided in $\sqrt{N} \times \sqrt{N}$ cells
- Number of cells for the inversion: $N = 324$ (discretization = $\lambda/6$)

Measurement domain:

- Total number of measurements: $M = 27$
- Measurement points placed on circles of radius $\rho = 3\lambda$

Sources:

- Plane waves
- Number of views: $V = 27$; $\theta_{inc}^v = 0^\circ + (v - 1) \times (360/V)$
- Amplitude: $A = 1.0$
- Frequency: $F = 300$ MHz ($\lambda = 1$)

Background:

- $\varepsilon_r = 1.0$
- $\sigma = 0$ [S/m]

Scatterer

- L-shaped object, $\ell = \lambda/2$
- $\varepsilon_r \in \{1.5, 2.0, 3.0\}$
- $\sigma = 0$ [S/m]

Born Iterative Method

- $I_{MAX} = 6$
- $\eta = 10^{-3}$

ELEDIA Research Center

1.4.1 L-shaped Object, $\ell = \lambda/2 - \tau = 0.5$

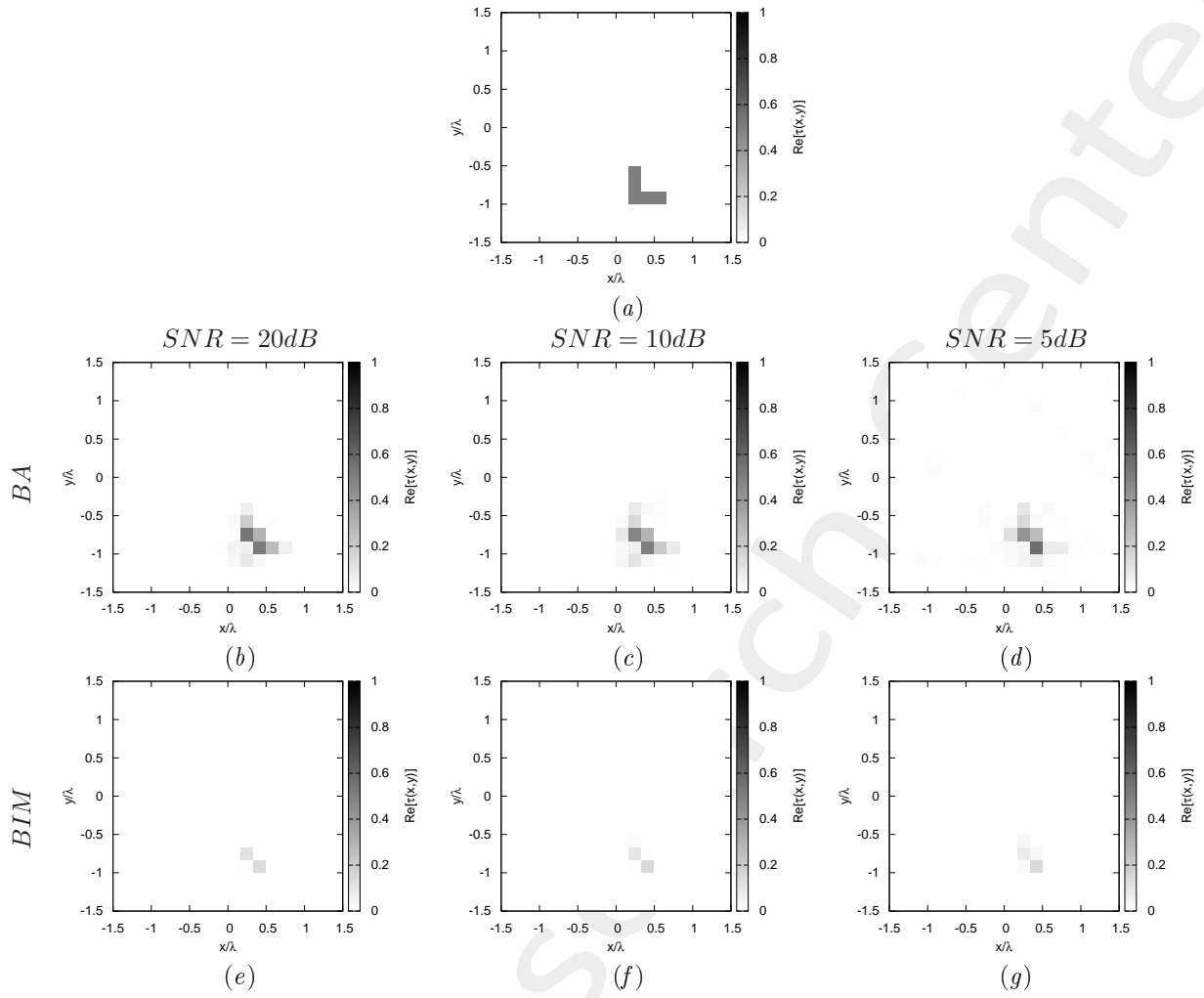


Figure 20: *L-shaped Object*, $\ell = \lambda/2$: (a) Direct problem with $\tau = 0.5$, (b)(e) ST-BCS reconstructed profiles for $SNR = 20$ [dB], (c)(f) $SNR = 10$ [dB] and (d)(g) $SNR = 5$ [dB] with (b)-(d) First Born approximation, (e)-(g) Born Iterative Method

1.4.2 L-shaped Object, $\ell = \lambda/2 - \tau = 1.0$

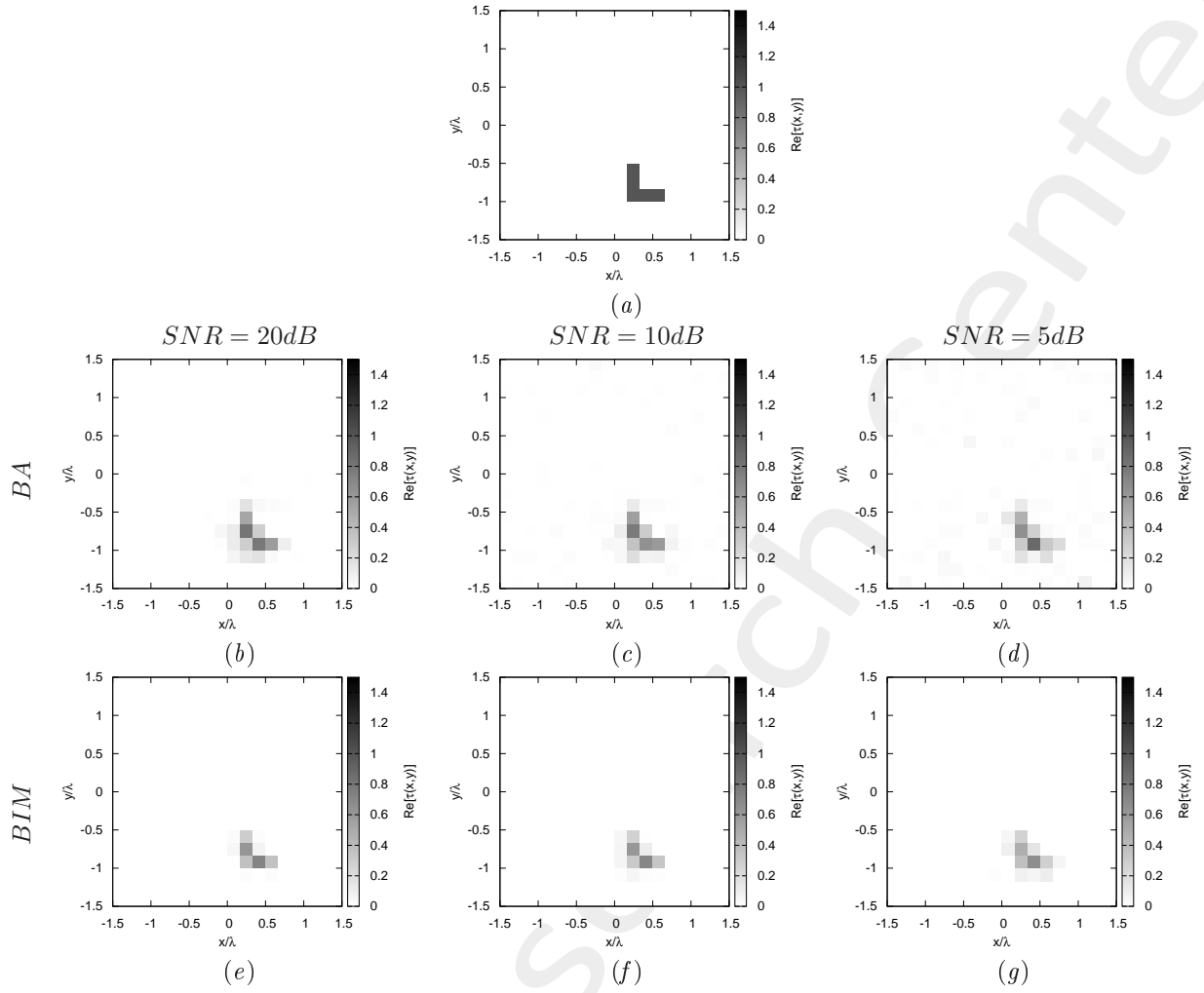


Figure 21: *L-shaped Object*, $\ell = \lambda/2$: (a) Direct problem with $\tau = 1.0$, (b)(e) ST-BCS reconstructed profiles for $SNR = 20$ [dB], (c)(f) $SNR = 10$ [dB] and (d)(g) $SNR = 5$ [dB] with (b)-(d) First Born approximation, (e)-(g) Born Iterative Method

	$SNR = 20dB$	$SNR = 10dB$	$SNR = 5dB$
Number of iterations	3	3	3

Table I: Number of steps before the break

1.4.3 L-shaped Object, $\ell = \lambda/2 - \tau = 2.0$

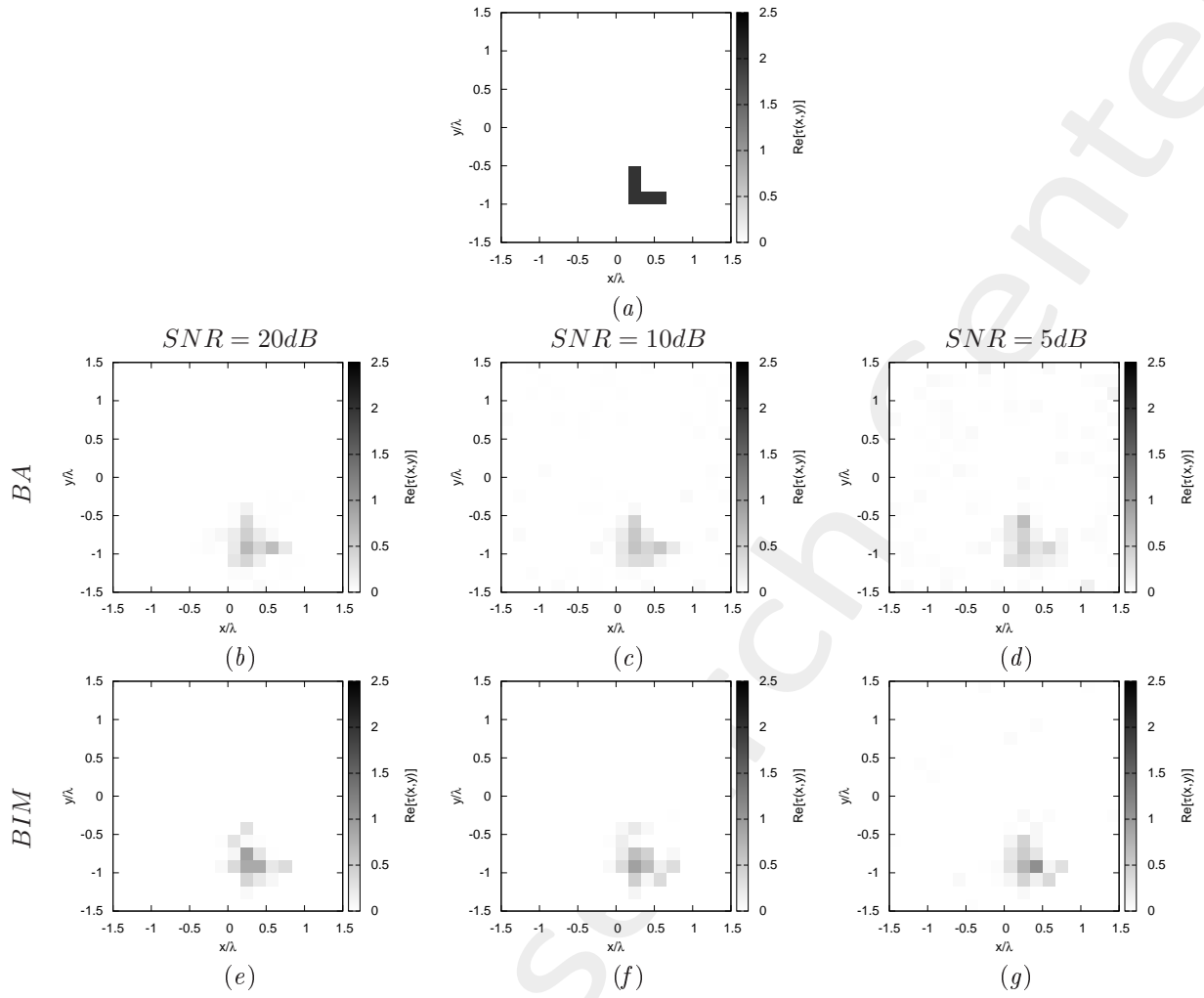


Figure 22: *L-shaped Object*, $\ell = \lambda/2$: (a) Direct problem with $\tau = 2.0$, (b)(e) ST-BCS reconstructed profiles for $SNR = 20$ [dB], (c)(f) $SNR = 10$ [dB] and (d)(g) $SNR = 5$ [dB] with (b)-(d) First Born approximation, (e)-(g) Born Iterative Method

1.5 E-shaped Object, $\ell_1 = \frac{5}{6}\lambda$, $\ell_2 = \lambda/2$

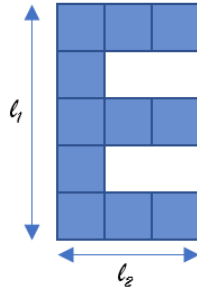


Figure 23: E-shaped Object

Test Case Description

Direct solver:

- Cubic domain divided in $\sqrt{D} \times \sqrt{D}$ cells
- Number of cells for the direct solver: $D = 1296$ (discretization = $\lambda/12$)

Inverse solver:

- Cubic domain divided in $\sqrt{N} \times \sqrt{N}$ cells
- Number of cells for the inversion: $N = 324$ (discretization = $\lambda/6$)

Measurement domain:

- Total number of measurements: $M = 27$
- Measurement points placed on circles of radius $\rho = 3\lambda$

Sources:

- Plane waves
- Number of views: $V = 27$; $\theta_{inc}^v = 0^\circ + (v - 1) \times (360/V)$
- Amplitude: $A = 1.0$
- Frequency: $F = 300$ MHz ($\lambda = 1$)

Background:

- $\varepsilon_r = 1.0$
- $\sigma = 0$ [S/m]

Scatterer

- E-shaped object, $\ell_1 = \frac{5}{6}\lambda$, $\ell_2 = \lambda/2$
- $\varepsilon_r \in \{1.5, 2.0, 3.0\}$
- $\sigma = 0$ [S/m]

Born Iterative Method

- $I_{MAX} = 6$
- $\eta = 10^{-3}$

ELEDIA Research Center

1.5.1 E-shaped Object, $\ell_1 = \frac{5}{6}\lambda$, $\ell_2 = \lambda/2 - \tau = 0.5$

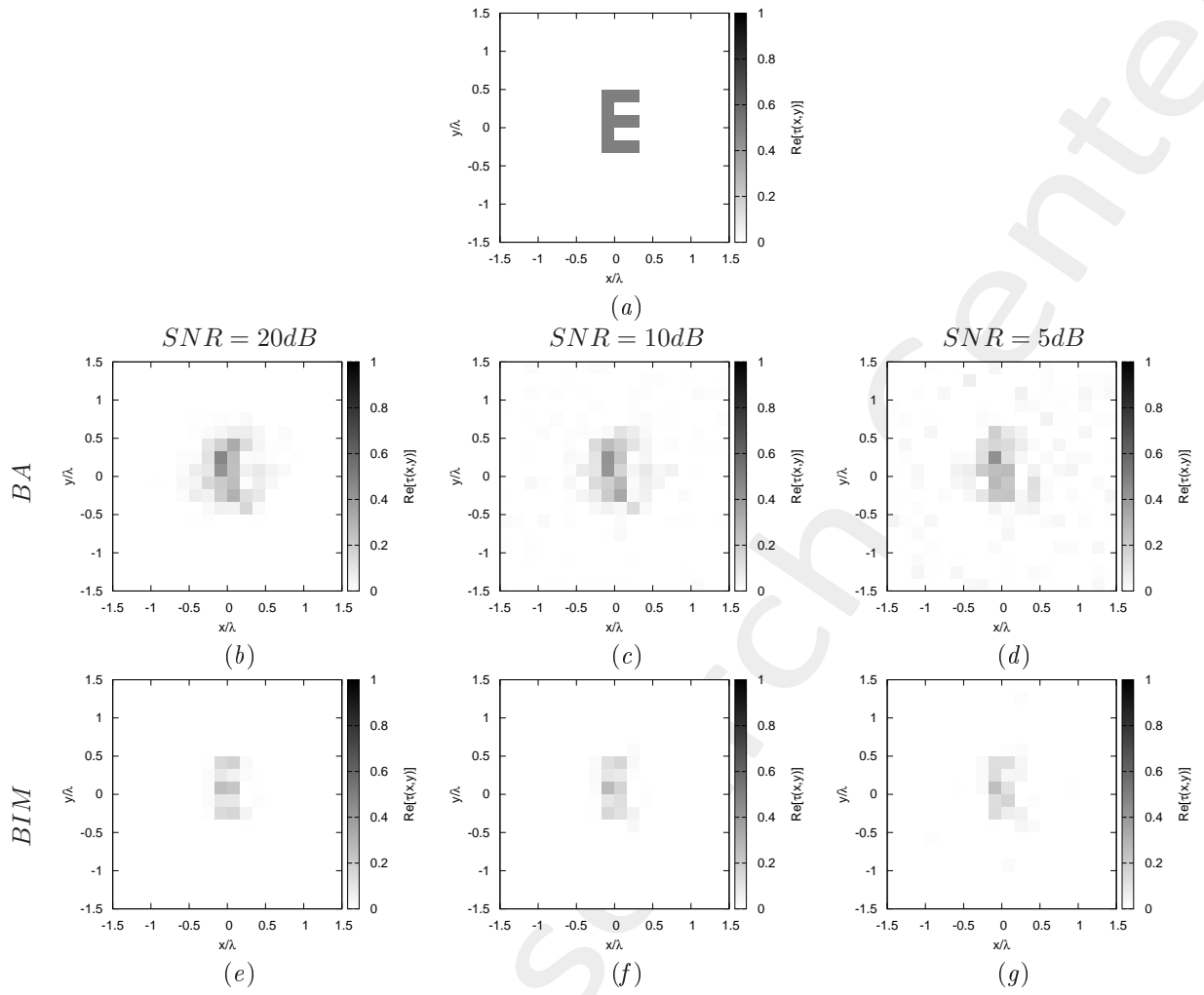


Figure 24: *E-shaped Object*, $\ell_1 = \frac{5}{6}\lambda$, $\ell_2 = \lambda/2$: (a) Direct problem with $\tau = 0.5$, (b) ST-BCS reconstructed profiles for $SNR = 20$ [dB], (c) $SNR = 10$ [dB] and (d) $SNR = 5$ [dB] with (b)-(d) First Born approximation, (e)-(g) Born Iterative Method

1.5.2 E-shaped Object, $\ell_1 = \frac{5}{6}\lambda$, $\ell_2 = \lambda/2$ - $\tau = 1.0$

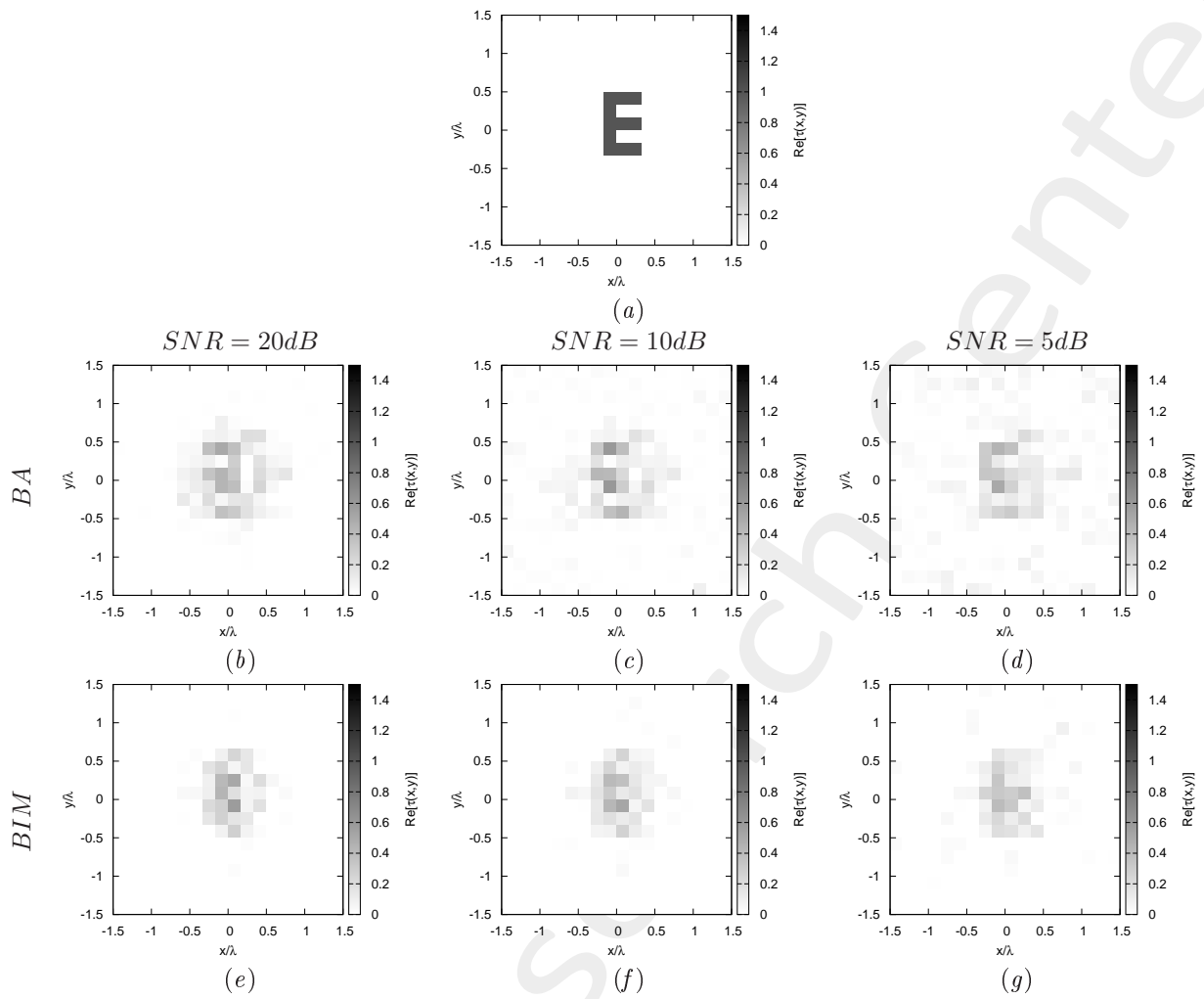


Figure 25: *E-shaped Object*, $\ell_1 = \frac{5}{6}\lambda$, $\ell_2 = \lambda/2$: (a) Direct problem with $\tau = 1.0$, (b)-(e) ST-BCS reconstructed profiles for $SNR = 20$ [dB], (c)(f) $SNR = 10$ [dB] and (d)(g) $SNR = 5$ [dB] with (b)-(d) First Born approximation, (e)-(g) Born Iterative Method

1.5.3 E-shaped Object, $\ell_1 = \frac{5}{6}\lambda$, $\ell_2 = \lambda/2 - \tau = 2.0$

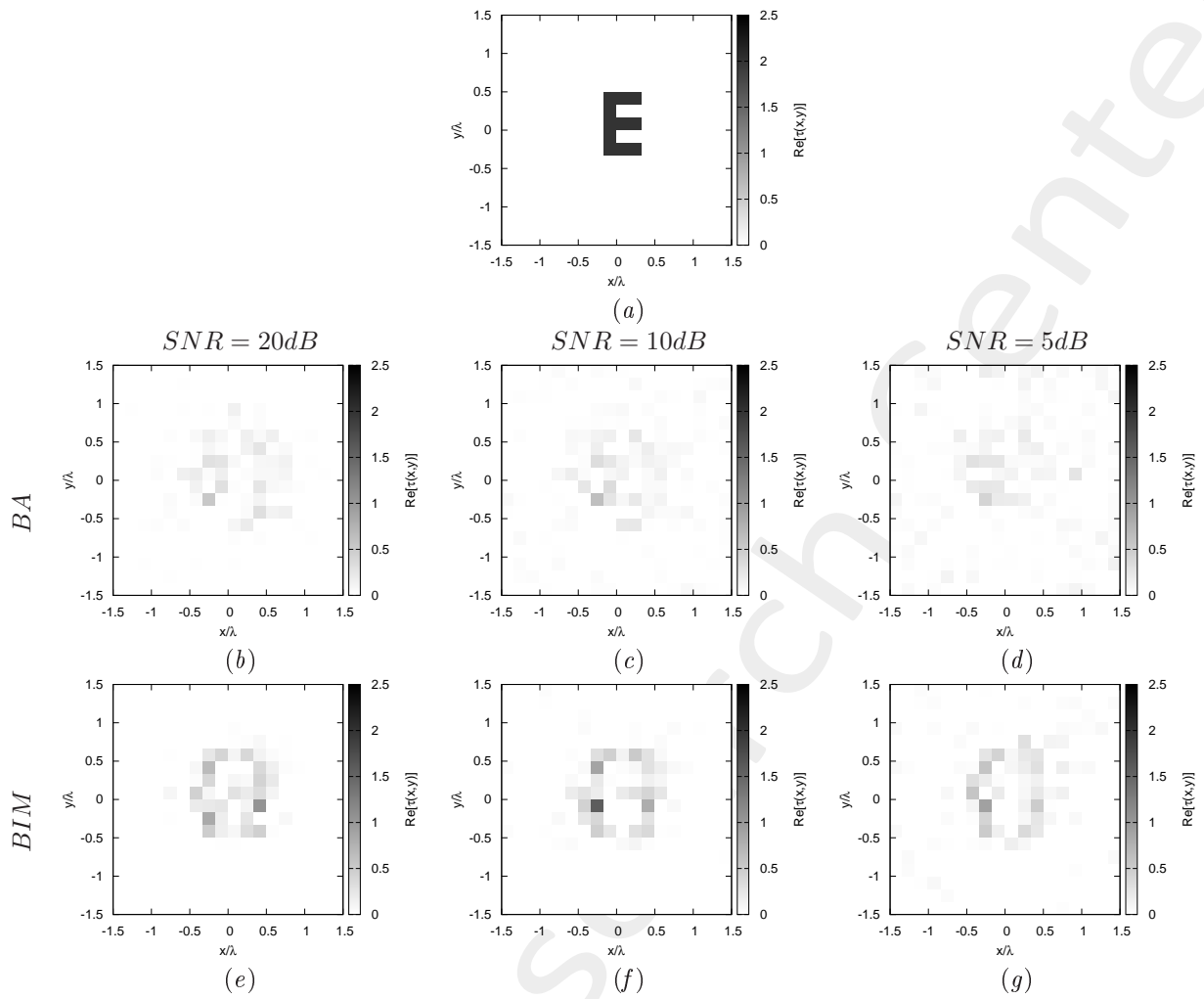


Figure 26: *E-shaped Object*, $\ell_1 = \frac{5}{6}\lambda$, $\ell_2 = \lambda/2$: (a) Direct problem with $\tau = 2.0$, (b)-(e) ST-BCS reconstructed profiles for $SNR = 20$ [dB], (c)(f) $SNR = 10$ [dB] and (d)(g) $SNR = 5$ [dB] with (b)-(d) First Born approximation, (e)-(g) Born Iterative Method

1.6 C-shaped Object, $l_1 = \frac{2}{3}\lambda$, $l_2 = \lambda/2$

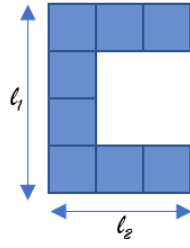


Figure 27: C-shaped Object

Test Case Description

Direct solver:

- Cubic domain divided in $\sqrt{D} \times \sqrt{D}$ cells
- Number of cells for the direct solver: $D = 1296$ (discretization = $\lambda/12$)

Inverse solver:

- Cubic domain divided in $\sqrt{N} \times \sqrt{N}$ cells
- Number of cells for the inversion: $N = 324$ (discretization = $\lambda/6$)

Measurement domain:

- Total number of measurements: $M = 27$
- Measurement points placed on circles of radius $\rho = 3\lambda$

Sources:

- Plane waves
- Number of views: $V = 27$; $\theta_{inc}^v = 0^\circ + (v - 1) \times (360/V)$
- Amplitude: $A = 1.0$
- Frequency: $F = 300$ MHz ($\lambda = 1$)

Background:

- $\varepsilon_r = 1.0$
- $\sigma = 0$ [S/m]

Scatterer

- C-shaped object, $\ell_1 = \frac{2}{3}\lambda$, $\ell_2 = \lambda/2$
- $\varepsilon_r \in \{1.5, 2.0, 3.0\}$
- $\sigma = 0$ [S/m]

Born Iterative Method

- $I_{MAX} = 6$
- $\eta = 10^{-3}$

ELEDIA Research Center

1.6.1 C-shaped Object, $\ell_1 = \frac{2}{3}\lambda$, $\ell_2 = \lambda/2$ - $\tau = 0.5$

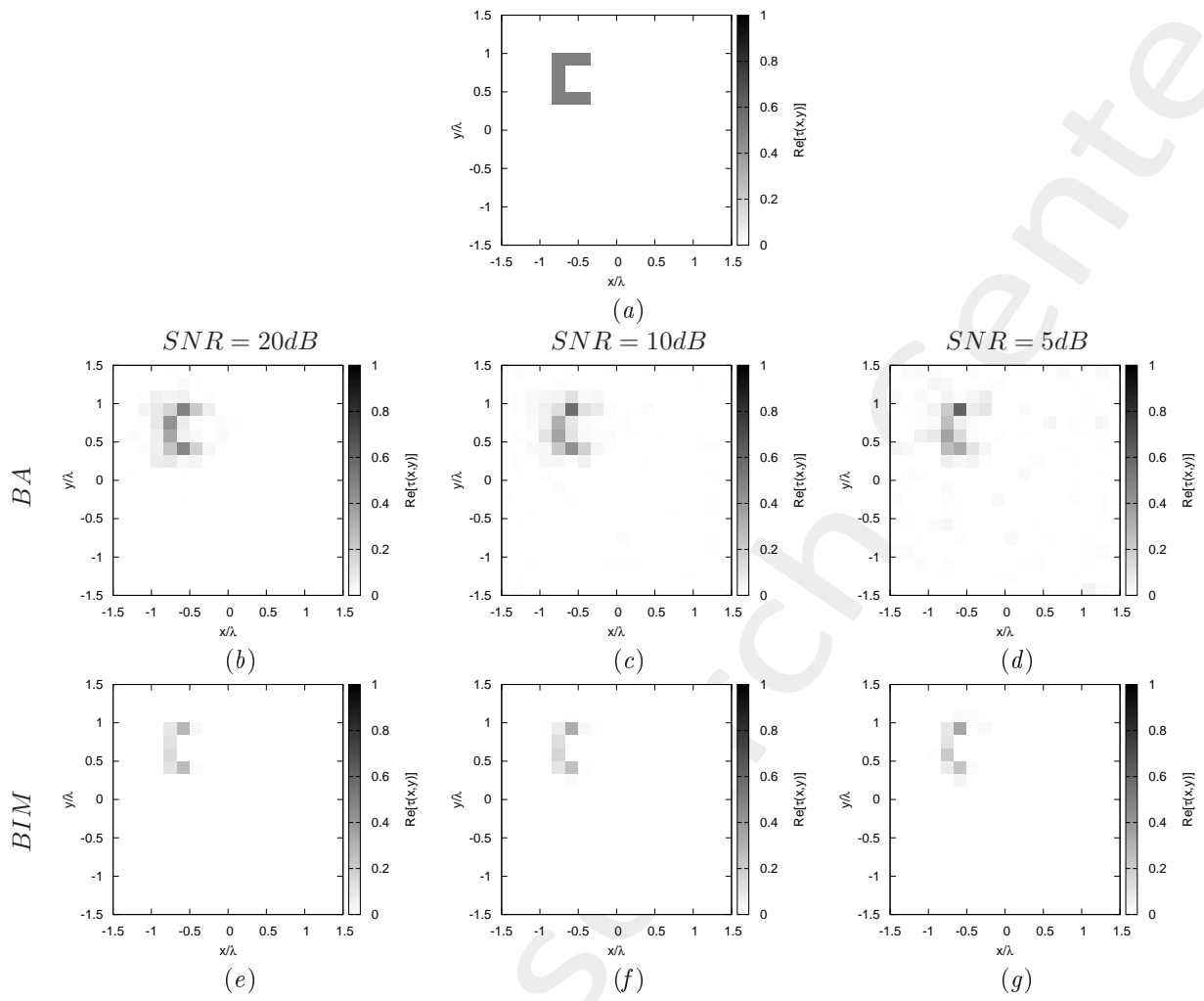


Figure 28: *C-shaped Object*, $\ell_1 = \frac{2}{3}\lambda$, $\ell_2 = \lambda/2$: (a) Direct problem with $\tau = 0.5$, (b) ST-BCS reconstructed profiles for $SNR = 20$ [dB], (c) $SNR = 10$ [dB] and (d) $SNR = 5$ [dB] with (b)-(d) First Born approximation, (e)-(g) Born Iterative Method

1.6.2 C-shaped Object, $\ell_1 = \frac{2}{3}\lambda$, $\ell_2 = \lambda/2$ - $\tau = 1.0$

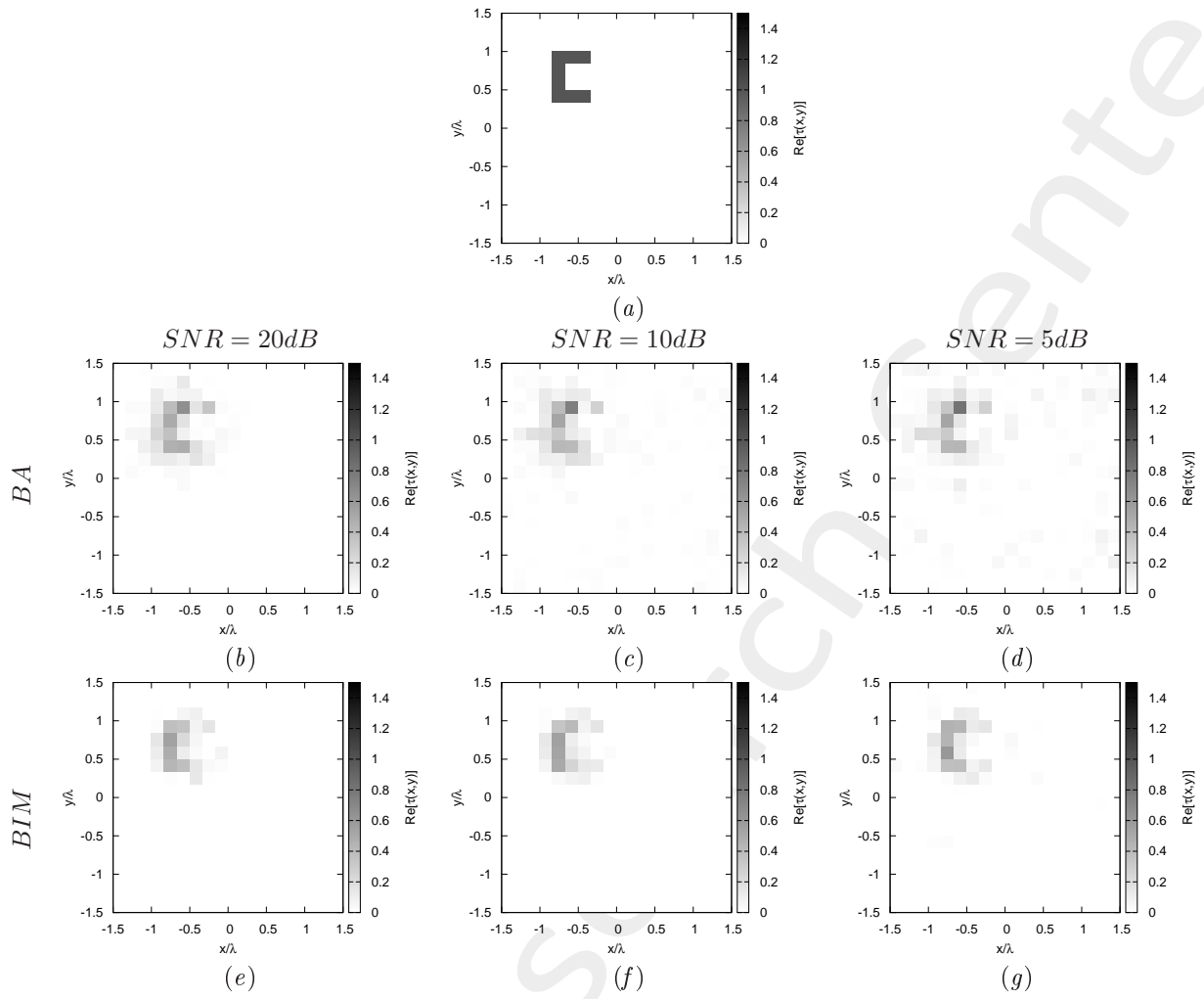


Figure 29: *C-shaped Object*, $\ell_1 = \frac{2}{3}\lambda$, $\ell_2 = \lambda/2$: (a) Direct problem with $\tau = 1.0$, (b)(e) ST-BCS reconstructed profiles for $SNR = 20$ [dB], (c)(f) $SNR = 10$ [dB] and (d)(g) $SNR = 5$ [dB] with (b)-(d) First Born approximation, (e)-(g) Born Iterative Method

1.6.3 C-shaped Object, $\ell_1 = \frac{2}{3}\lambda$, $\ell_2 = \lambda/2 - \tau = 2.0$

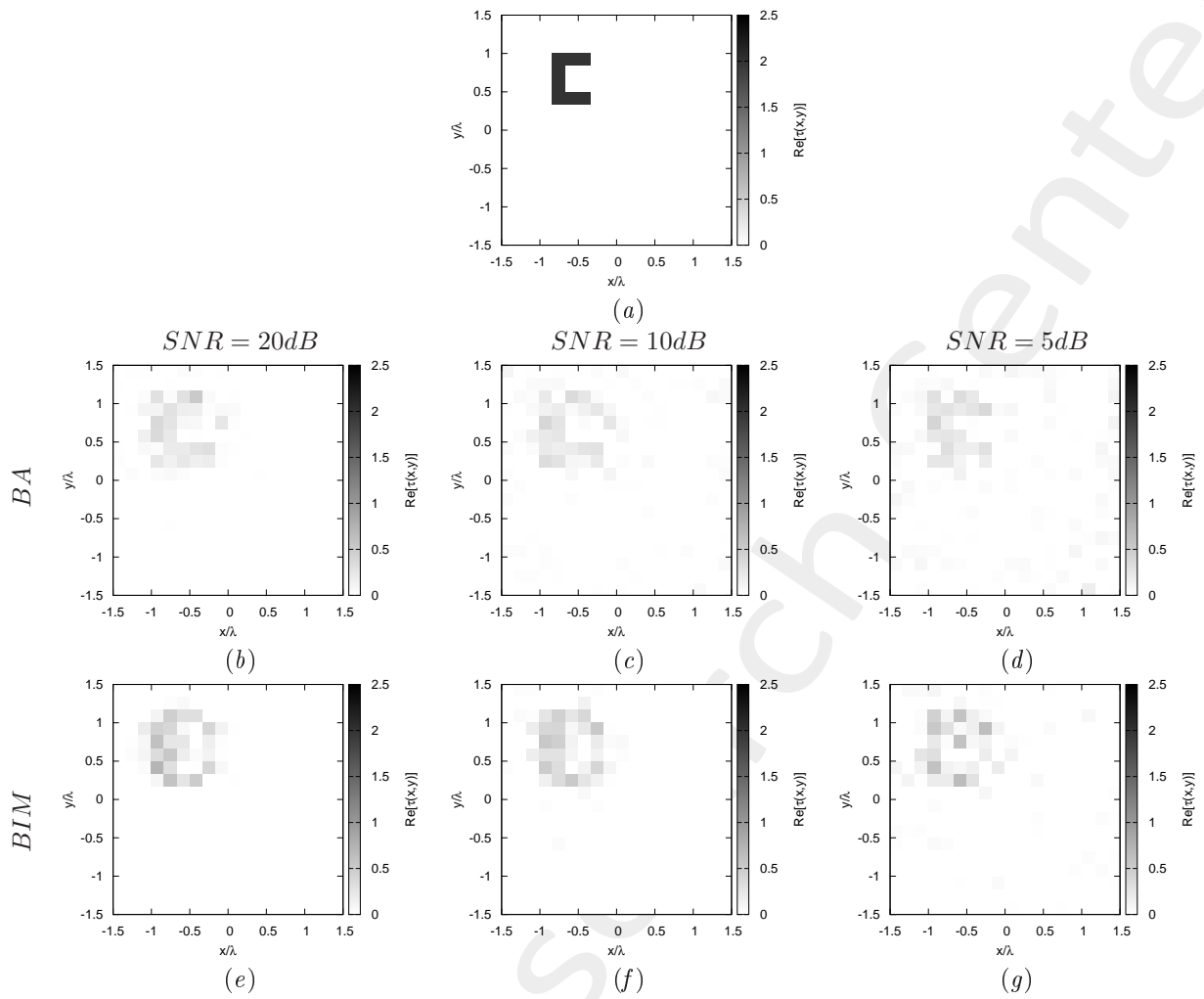


Figure 30: *C-shaped Object*, $\ell_1 = \frac{2}{3}\lambda$, $\ell_2 = \lambda/2$: (a) Direct problem with $\tau = 2.0$, (b)(e) ST-BCS reconstructed profiles for $SNR = 20$ [dB], (c)(f) $SNR = 10$ [dB] and (d)(g) $SNR = 5$ [dB] with (b)-(d) First Born approximation, (e)-(g) Born Iterative Method

1.7 Rectangle-shaped Object, $\ell = \lambda/2$, $h = \lambda/3$

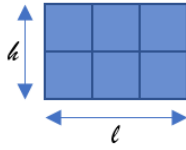


Figure 31: Rectangle-shaped Object

Test Case Description

Direct solver:

- Cubic domain divided in $\sqrt{D} \times \sqrt{D}$ cells
- Number of cells for the direct solver: $D = 1296$ (discretization = $\lambda/12$)

Inverse solver:

- Cubic domain divided in $\sqrt{N} \times \sqrt{N}$ cells
- Number of cells for the inversion: $N = 324$ (discretization = $\lambda/6$)

Measurement domain:

- Total number of measurements: $M = 27$
- Measurement points placed on circles of radius $\rho = 3\lambda$

Sources:

- Plane waves
- Number of views: $V = 27$; $\theta_{inc}^v = 0^\circ + (v - 1) \times (360/V)$
- Amplitude: $A = 1.0$
- Frequency: $F = 300$ MHz ($\lambda = 1$)

Background:

- $\varepsilon_r = 1.0$
- $\sigma = 0$ [S/m]

Scatterer

- Rectangle-shaped object, $\ell = \lambda/2$, $h = \lambda/3$
- $\varepsilon_r \in \{1.5, 2.0, 3.0\}$
- $\sigma = 0$ [S/m]

Born Iterative Method

- $I_{MAX} = 6$
- $\eta = 10^{-3}$

ELEDIA Research Center

1.7.1 Rectangle-shaped Object, $\ell = \lambda/2$, $h = \lambda/3$ - $\tau = 0.5$

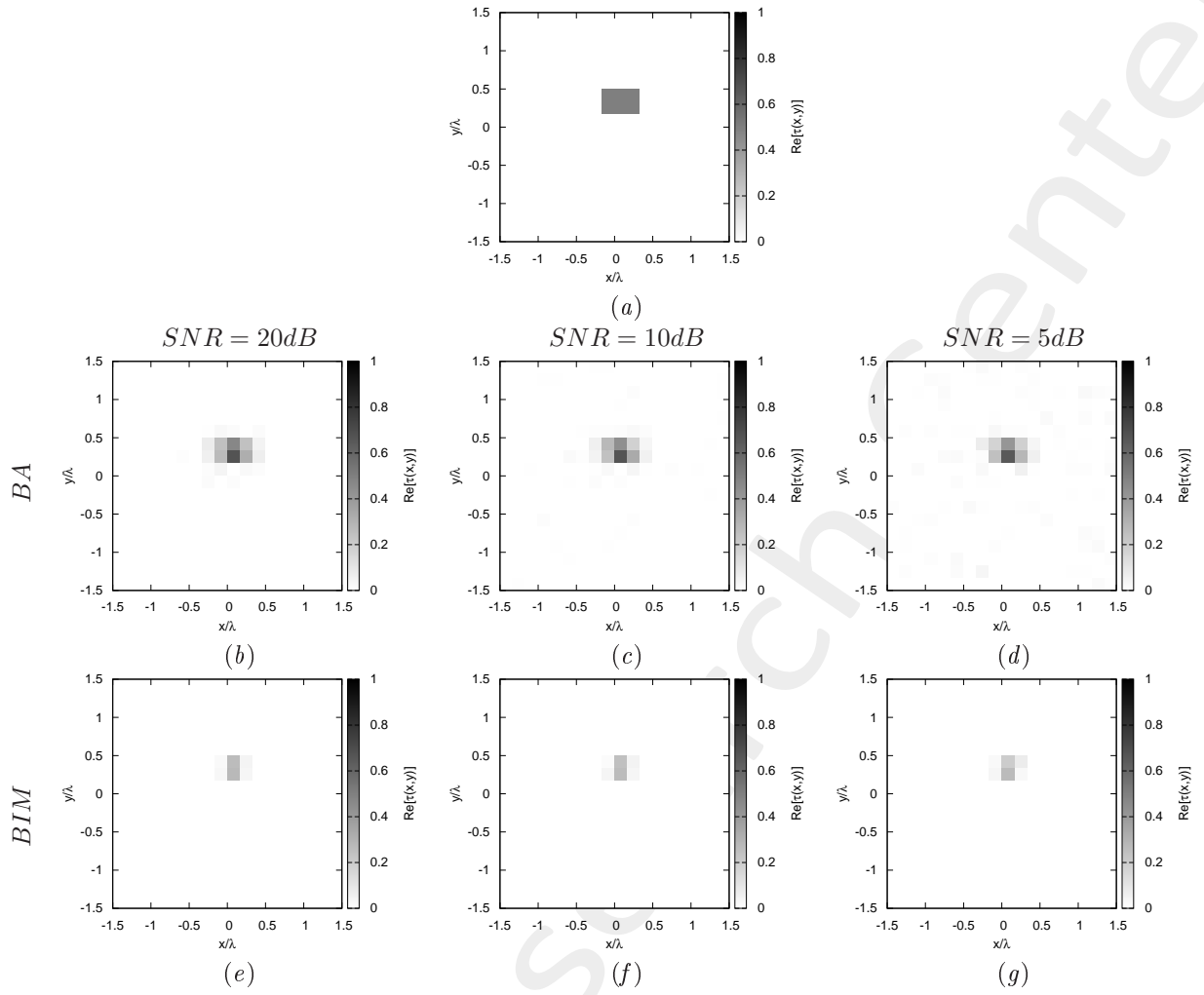


Figure 32: *Rectangle-shaped Object*, $\ell = \lambda/2$, $h = \lambda/3$: (a) Direct problem with $\tau = 0.5$, (b) ST-BCS reconstructed profiles for $SNR = 20$ [dB], (c) $SNR = 10$ [dB] and (d) $SNR = 5$ [dB] with (b)-(d) First Born approximation, (e)-(g) Born Iterative Method

1.7.2 Rectangle-shaped Object, $\ell = \lambda/2$, $h = \lambda/3$ - $\tau = 1.0$

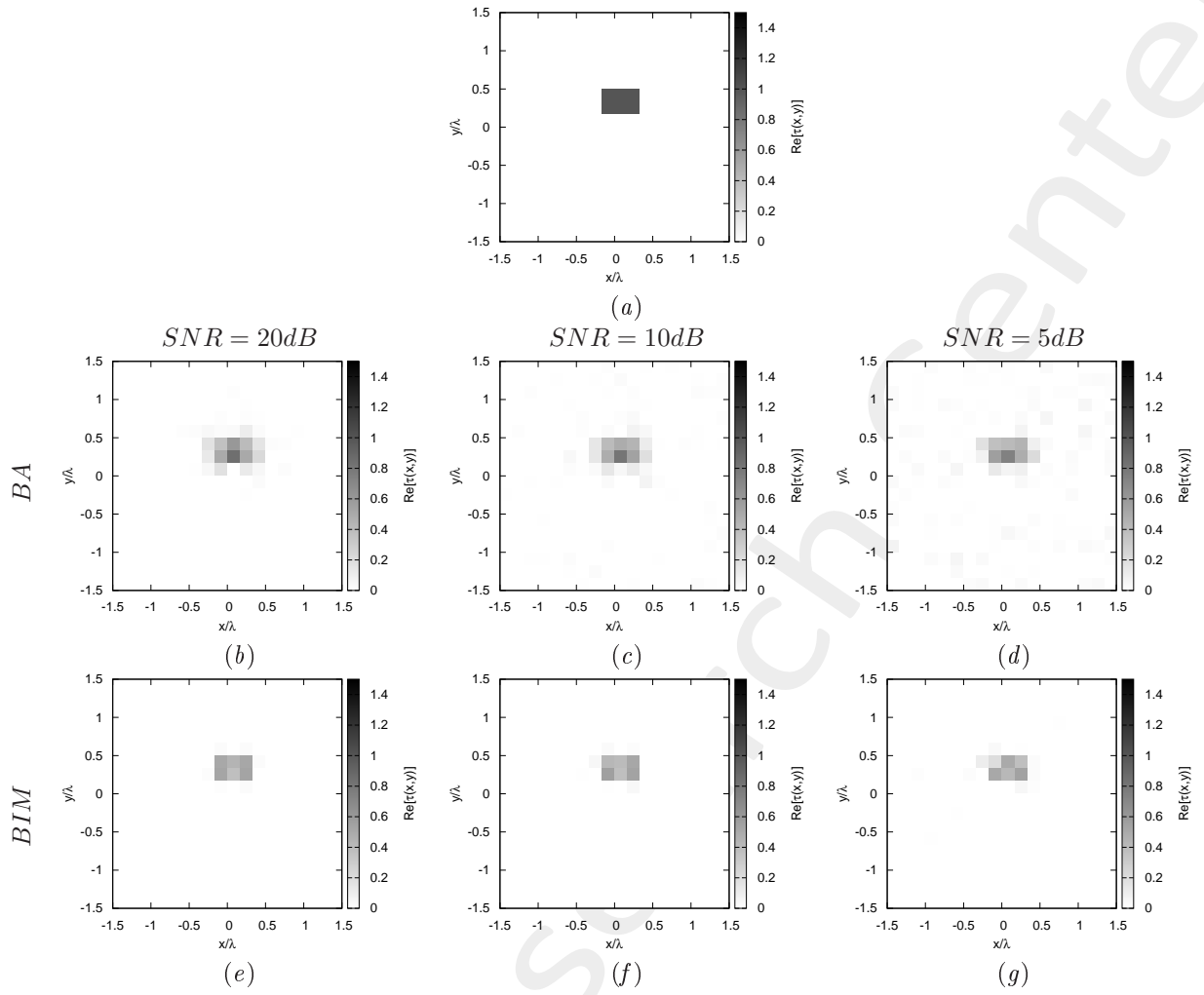


Figure 33: *Rectangle-shaped Object*, $\ell = \lambda/2$, $h = \lambda/3$: (a) Direct problem with $\tau = 1.0$, (b)(e) ST-BCS reconstructed profiles for $SNR = 20$ [dB], (c)(f) $SNR = 10$ [dB] and (d)(g) $SNR = 5$ [dB] with (b)-(d) First Born approximation, (e)-(g) Born Iterative Method

1.7.3 Rectangle-shaped Object, $\ell = \lambda/2$, $h = \lambda/3$ - $\tau = 2.0$

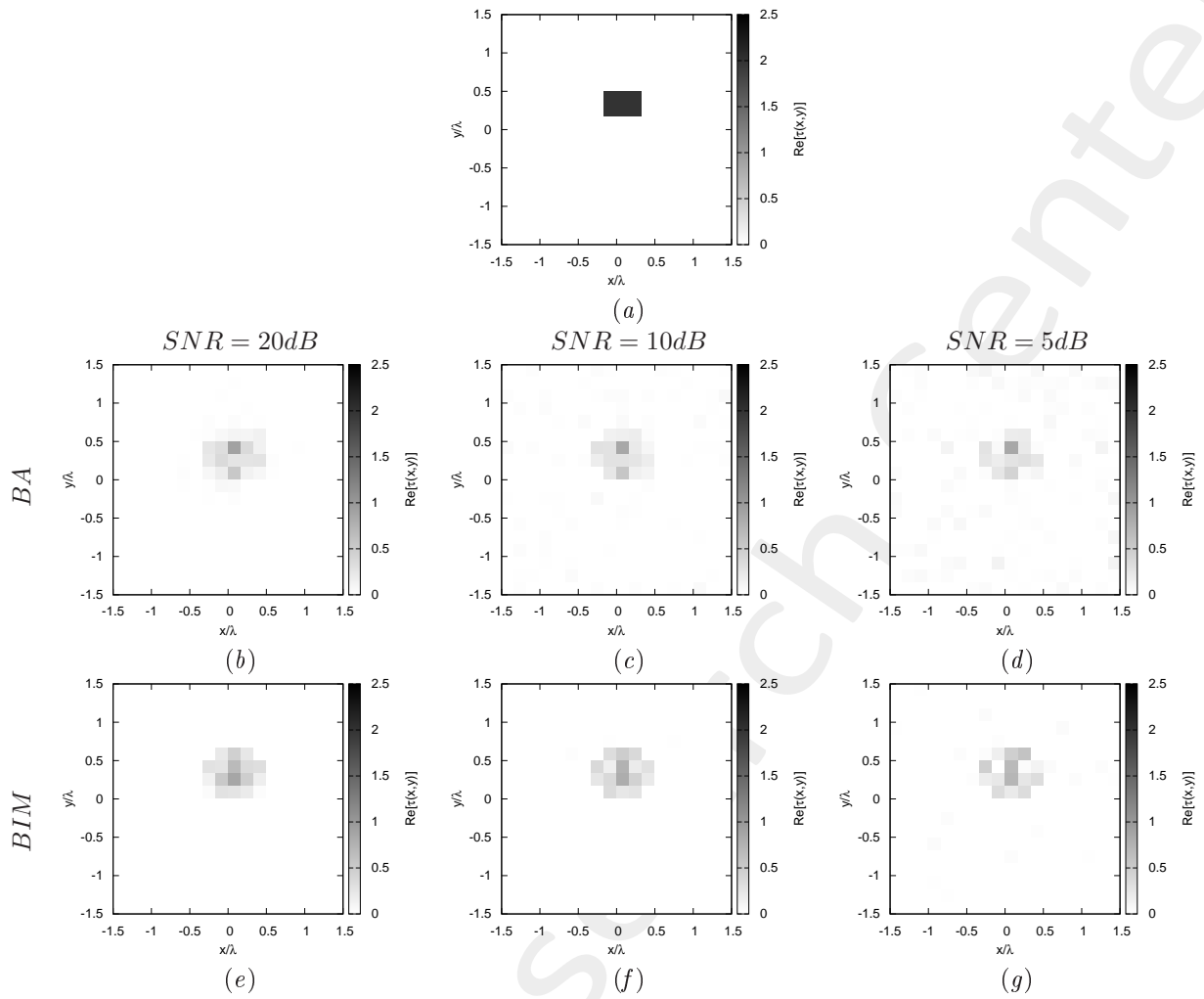


Figure 34: *Rectangle-shaped Object*, $\ell = \lambda/2$, $h = \lambda/3$: (a) Direct problem with $\tau = 2.0$, (b)(e) ST-BCS reconstructed profiles for $SNR = 20$ [dB], (c)(f) $SNR = 10$ [dB] and (d)(g) $SNR = 5$ [dB] with (b)-(d) First Born approximation, (e)-(g) Born Iterative Method

1.8 Multiple Objects

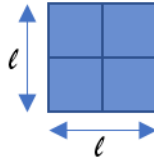


Figure 35: Square-shaped Object

Test Case Description

Direct solver:

- Cubic domain divided in $\sqrt{D} \times \sqrt{D}$ cells
- Number of cells for the direct solver: $D = 1296$ (discretization = $\lambda/12$)

Inverse solver:

- Cubic domain divided in $\sqrt{N} \times \sqrt{N}$ cells
- Number of cells for the inversion: $N = 324$ (discretization = $\lambda/6$)

Measurement domain:

- Total number of measurements: $M = 27$
- Measurement points placed on circles of radius $\rho = 3\lambda$

Sources:

- Plane waves
- Number of views: $V = 27$; $\theta_{inc}^v = 0^\circ + (v - 1) \times (360/V)$
- Amplitude: $A = 1.0$
- Frequency: $F = 300$ MHz ($\lambda = 1$)

Background:

- $\epsilon_r = 1.0$
- $\sigma = 0$ [S/m]

Scatterer

- 3 Square-shaped object, $\ell = \lambda/3$
- $\varepsilon_r \in \{1.5, 2.0, 3.0\}$
- $\sigma = 0$ [S/m]

Born Iterative Method

- $I_{MAX} = 6$
- $\eta = 10^{-3}$

ELEDIA Research Center

1.8.1 Multiple Objects, $\tau = 0.5$

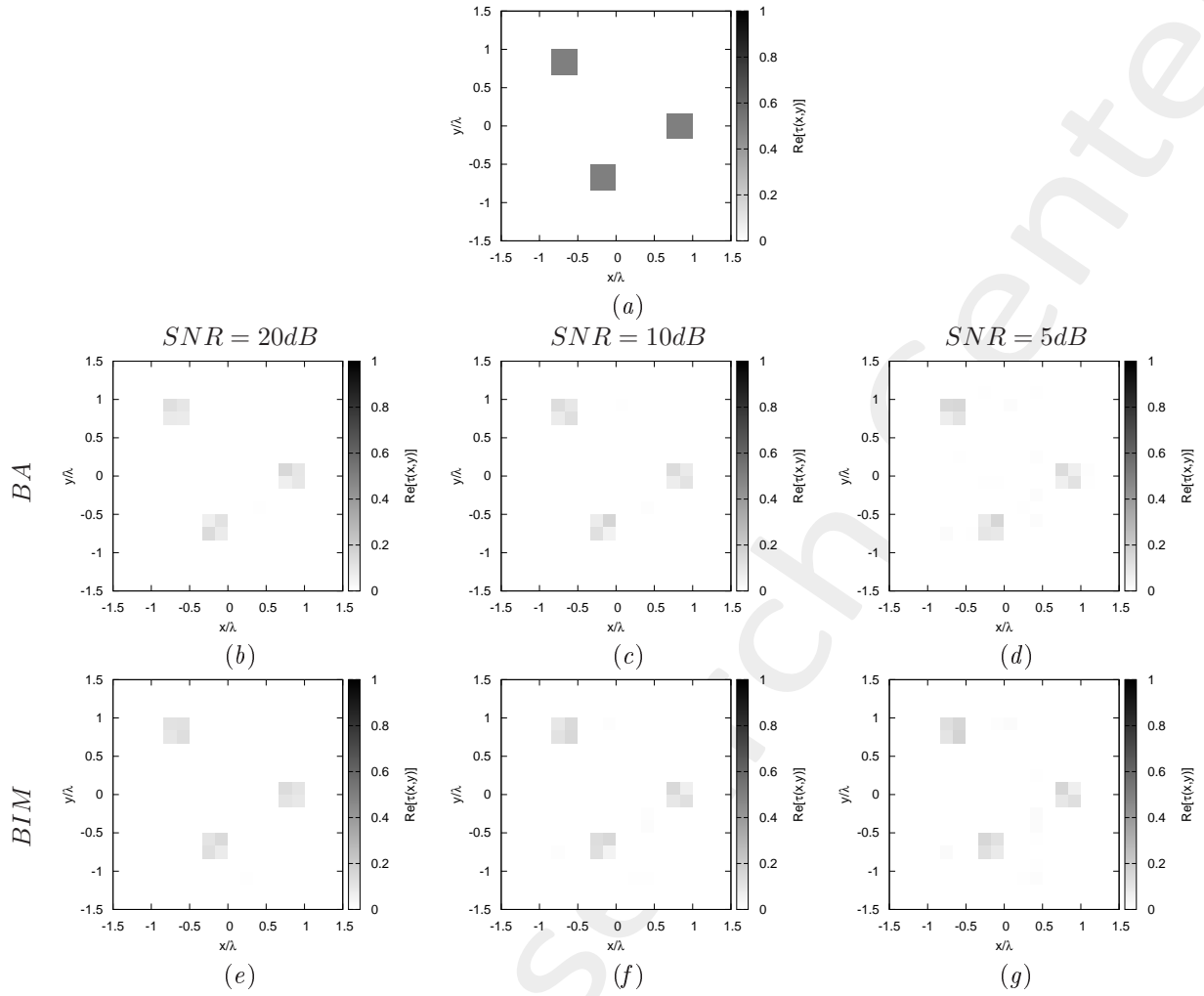


Figure 36: *Multiple Objects, 3 square-shaped Objects: $\ell = \lambda/3$: (a) Direct problem with $\tau = 0.5$, (b) ST-BCS reconstructed profiles for $SNR = 20$ [dB], (c) $SNR = 10$ [dB] and (d) $SNR = 5$ [dB] with (b)-(d) First Born approximation, (e)-(g) Born Iterative Method*

1.8.2 Multiple Object, $\tau = 1.0$

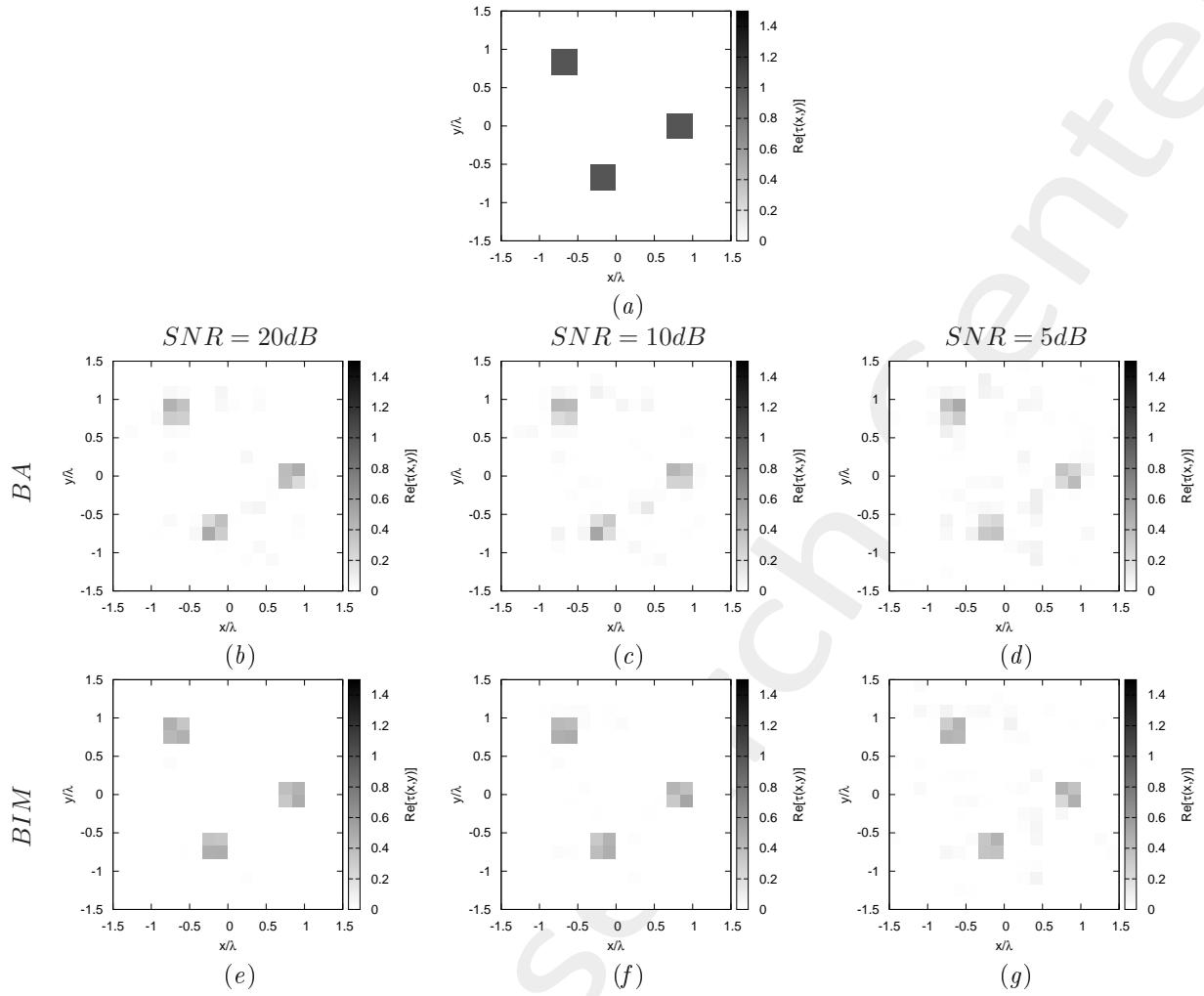


Figure 37: *Multiple Objects, 3 square-shaped Objects: $\ell = \lambda/3$: (a) Direct problem with $\tau = 1.0$, (b)(e) ST-BCS reconstructed profiles for $SNR = 20$ [dB], (c)(f) $SNR = 10$ [dB] and (d)(g) $SNR = 5$ [dB] with (b)-(d) First Born approximation, (e)-(g) Born Iterative Method*

1.8.3 Multiple Objects, $\tau = 2.0$

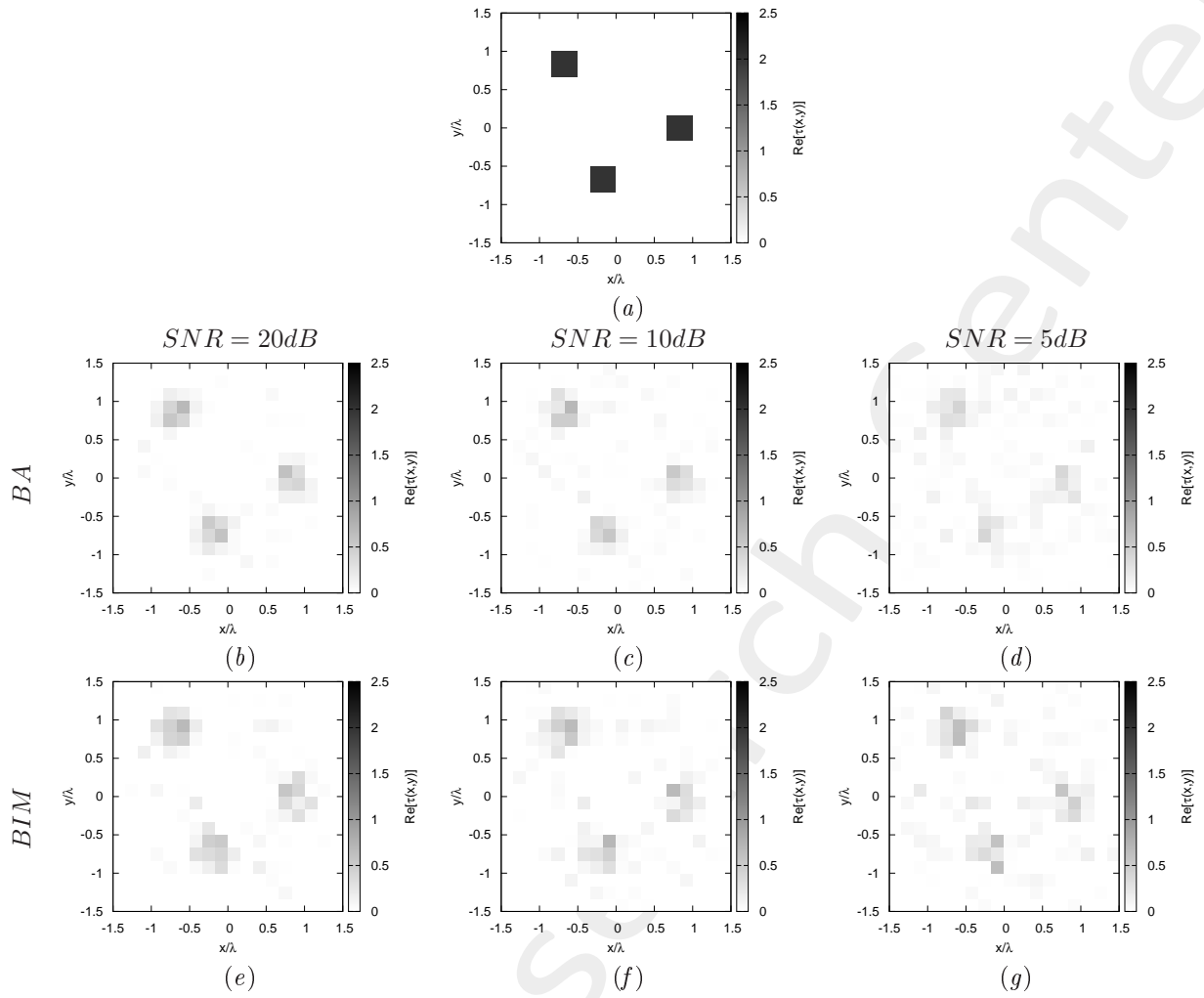


Figure 38: *Multiple Objects, 3 square-shaped Objects: $\ell = \lambda/3$: (a) Direct problem with $\tau = 2.0$, (b)(e) ST-BCS reconstructed profiles for $SNR = 20$ [dB], (c)(f) $SNR = 10$ [dB] and (d)(g) $SNR = 5$ [dB] with (b)-(d) First Born approximation, (e)-(g) Born Iterative Method*

References

- [1] G. Oliveri, M. Salucci, N. Anselmi, and A. Massa, "Compressive sensing as applied to inverse problems for imaging: theory, applications, current trends, and open challenges," *IEEE Antennas Propag. Mag.*, vol. 59, no. 5, pp. 34-46, Oct. 2017.
- [2] A. Massa, P. Rocca, and G. Oliveri, "Compressive sensing in electromagnetics - A review," *IEEE Antennas Propag. Mag.*, pp. 224-238, vol. 57, no. 1, Feb. 2015.
- [3] G. Oliveri, L. Poli, N. Anselmi, M. Salucci, and A. Massa, "Compressive sensing-based Born iterative method for tomographic imaging," *IEEE Trans. Microw. Theory Techn.*, vol. 67, no. 5, pp. 1753-1765, May 2019.
- [4] M. Salucci, A. Gelmini, L. Poli, G. Oliveri, and A. Massa, "Progressive compressive sensing for exploiting frequency-diversity in GPR imaging," *Journal of Electromagnetic Waves and Applications*, vol. 32, no. 9, pp. 1164-1193, 2018.
- [5] N. Anselmi, L. Poli, G. Oliveri, and A. Massa, "Iterative multi-resolution bayesian CS for microwave imaging," *IEEE Trans. Antennas Propag.*, vol. 66, no. 7, pp. 3665-3677, Jul. 2018.
- [6] N. Anselmi, G. Oliveri, M. A. Hannan, M. Salucci, and A. Massa, "Color compressive sensing imaging of arbitrary-shaped scatterers," *IEEE Trans. Microw. Theory Techn.*, vol. 65, no. 6, pp. 1986-1999, Jun. 2017.
- [7] N. Anselmi, G. Oliveri, M. Salucci, and A. Massa, "Wavelet-based compressive imaging of sparse targets," *IEEE Trans. Antennas Propag.*, vol. 63, no. 11, pp. 4889-4900, Nov. 2015.
- [8] G. Oliveri, N. Anselmi, and A. Massa, "Compressive sensing imaging of non-sparse 2D scatterers by a total-variation approach within the Born approximation," *IEEE Trans. Antennas Propag.*, vol. 62, no. 10, pp. 5157-5170, Oct. 2014.
- [9] L. Poli, G. Oliveri, and A. Massa, "Imaging sparse metallic cylinders through a local shape function Bayesian compressive sensing approach," *Journal of Optical Society of America A*, vol. 30, no. 6, pp. 1261-1272, 2013.
- [10] L. Poli, G. Oliveri, F. Viani, and A. Massa, "MT-BCS-based microwave imaging approach through minimum-norm current expansion," *IEEE Trans. Antennas Propag.*, vol. 61, no. 9, pp. 4722-4732, Sep. 2013.
- [11] L. Poli, G. Oliveri, P. Rocca, and A. Massa, "Bayesian compressive sensing approaches for the reconstruction of two-dimensional sparse scatterers under TE illumination," *IEEE Trans. Geosci. Remote Sens.*, vol. 51, no. 5, pp. 2920-2936, May 2013.
- [12] L. Poli, G. Oliveri, and A. Massa, "Microwave imaging within the first-order Born approximation by means of the contrast-field Bayesian compressive sensing," *IEEE Trans. Antennas Propag.*, vol. 60, no. 6, pp. 2865-2879, Jun. 2012.

- [13] G. Oliveri, L. Poli, P. Rocca, and A. Massa, "Bayesian compressive optical imaging within the Rytov approximation," *Optics Letters*, vol. 37, no. 10, pp. 1760-1762, 2012.
- [14] G. Oliveri, P. Rocca, and A. Massa, "A Bayesian compressive sampling-based inversion for imaging sparse scatterers," *IEEE Trans. Geosci. Remote Sens.*, vol. 49, no. 10, pp. 3993-4006, Oct. 2011.
- [15] M. Salucci, A. Gelmini, G. Oliveri, and A. Massa, "Planar arrays diagnosis by means of an advanced Bayesian compressive processing," *IEEE Trans. Antennas Propag.*, vol. 66, no. 11, pp. 5892-5906, Nov. 2018.
- [16] L. Poli, G. Oliveri, P. Rocca, M. Salucci, and A. Massa, "Long-distance WPT unconventional arrays synthesis," *Journal of Electromagnetic Waves and Applications*, vol. 31, no. 14, pp. 1399-1420, Jul. 2017.
- [17] G. Oliveri, M. Salucci, and A. Massa, "Synthesis of modular contiguously clustered linear arrays through a sparseness-regularized solver," *IEEE Trans. Antennas Propag.*, vol. 64, no. 10, pp. 4277-4287, Oct. 2016.
- [18] P. Rocca, M. A. Hannan, M. Salucci, and A. Massa, "Single-snapshot DoA estimation in array antennas with mutual coupling through a multi-scaling BCS strategy," *IEEE Trans. Antennas Propag.*, vol. 65, no. 6, pp. 3203-3213, Jun. 2017.
- [19] M. Salucci, L. Poli, and G. Oliveri, "Full-vectorial 3D microwave imaging of sparse scatterers through a multi-task Bayesian compressive sensing approach," *Journal of Imaging*, vol. 5, no. 1, pp. 1-24, Jan. 2019 (DOI: 10.3390/jimaging5010019).